Photometric Study of the Kreutz Comets Observed by SOHO from 1996–2005

Matthew M. Knight[1,2], Michael F. A'Hearn[3], Douglas A. Biesecker[4], Guillaume Faury[5], Douglas P. Hamilton[3], Philippe Lamy[5], Antoine Llebaria[5]

Contacting author: knight@lowell.edu

Astronomical Journal draft v1.0

March 27, 2009

Manuscript pages: 105 double spaced

6 tables

19 figures

[1]Lowell Observatory, 1400 W. Mars Hill Rd, Flagstaff, AZ 86001

[2]Work completed while at the University of Maryland.

[3]Department of Astronomy, University of Maryland, College Park, MD 20742-2421

[4]NOAA Space Weather Prediction Center, 325 Broadway, Boulder, CO 80305

[5]Laboratoire d'Astronomie Spatiale, 38 rue Frederic Joliot-Curie, 13388 Marseille Cedex 13, France

Proposed running head: SOHO Observed Kreutz Comets 1996–2005

Please address all editorial correspondence and proofs to:

Matthew M. Knight

Lowell Observatory

1400 W. Mars Hill Rd

Flagstaff, AZ 86001

knight@lowell.edu

Office: 928-774-3358

Fax: 928-774-6296

Abstract

We present the photometry of the more than 900 Kreutz comets observed by SOHO from 1996–2005. The Kreutz comets have "sungrazing" orbits with q≈1–2 $R_\odot$, high inclinations (i≈143°), and periods of 500–1000 years. We find that they do not have a bimodal distance of peak brightness as previously reported, but instead peak from 10.5–14 $R_\odot$ (prior to perihelion), suggesting there is a continuum of compositions rather than two distinct subpopulations. The lightcurves have two rates of brightening, typically $\propto r^{-7.3\pm2.0}$ when first observed by SOHO then rapidly transitioning to $\propto r^{-3.8\pm0.7}$ between 20–30 $R_\odot$. It is unclear at what distance the steeper slope begins, but it likely does not extend much beyond the SOHO field of view. We derive nuclear sizes up to ∼50 meters in radius for the SOHO observed comets, with a cumulative size distribution of $N(>R)\propto R^{-2.2}$ for comets larger than 5 meters in radius. This size distribution cannot explain the six largest members of the family seen from the ground, suggesting that either the size distribution does not extend to the largest sizes or that the distribution is not uniform around the orbit. The total mass of the distribution up to the largest expected size (∼500 meters) is $\sim4\times10^{14}$ g, much less than the estimated mass of the largest ground observed members. After correcting for the changing discovery circumstances, the flux of comets reaching perihelion has increased since 1996, and the increase is seen in comets of all sizes. Comparison of the SOHO comets with the Solwind and SMM discoveries suggests there was an over-abundance of bright comets arriving from 1979–1989, possibly indicative of a changing distribution around the Kreutz orbit.

This research was supported by NASA Planetary Atmospheres grants NAG513295 and NNG06GF29G.

Keywords: Comets, Kreutz, SOHO, Sungrazing

1. Introduction

The Kreutz group of sungrazing comets has included some of the most spectacular comets on record, including the "Great Comet of 1106" (X/1106 C1), the "Great Comet of 1882" (1882 II = 1882b = C/1882 R1), and Ikeya-Seki (1965 VIII = 1965f = C/1965 S1). The group was first recognized by Kirkwood (1880) and Kreutz (1888, 1891, 1901) on the basis of similar orbits of several comets from the 1600s and 1800s. As additional group members were observed in 1943, 1963, 1965, and 1970, Marsden (1967), Hasegawa (1966), Kresák (1966), Sekanina (1967b,a), and others updated and expanded the analysis of the Kreutz group. The discovery of 16 fainter Kreutz comets from 1979–1989 (and three more in archival images since then) by the space-based coronagraphs Solar Maximum Mission (SMM) and Solwind (Sheeley et al. 1982; Michels et al. 1982; Weissman 1983; Marsden 1989; MacQueen & St. Cyr 1991) and the hundreds of Kreutz comets discovered by SOHO (Raymond et al. 1998; Uzzo et al. 2001; Biesecker et al. 2002) (as well as a handful discovered by STEREO) have renewed interest in the Kreutz group.

Much of this work has focused on the orbital dynamics of the largest members of the group. It has been well established that the two most prominent members, Ikeya-Seki and the Great Comet of 1882 split from each other very close to perihelion around the year 1100 CE (e.g. Marsden (1967), Sekanina & Chodas (2002a)) and were quite possibly observed as the magnificent comet of 1106. While the fragmentation history of the remaining ground observed comets is not well understood, it is likely that they split from one or more parent fragments at some time prior to the 1500s, and that all of these parent fragments (including the parent of the Great Comet of 1882 and Ikeya-Seki) split from a single progenitor within the last 2500 years (Sekanina & Chodas 2002b, 2004, 2007, 2008). Sekanina & Chodas (2007) envision the Kreutz group to be much more populous than previously suggested, incorporating more than 20 poorly observed near-Sun comets recovered from the historical

records by Hasegawa & Nakano (2001), Strom (2002), and England (2002), and potentially linking the progenitor with comets observed in 214 BCE, 423 CE, and/or 467 CE.

The Solwind, SMM, SOHO, and STEREO discovered comets are not sufficiently well observed to permit investigation of the dynamical history of individual comets. Instead, it has been demonstrated through statistical arguments (Sekanina 2000a, 2002a,b) that these comets are likely products of runaway fragmentation throughout their orbits. In these models, the small coronagraphically discovered comets all split from their parent fragments since the previous perihelion passage. These fragmentation events occurred both before and after aphelion, at distances small and large. Splitting is likely to have continued in the newly produced fragments with increasing time between subsequent events. Thus, the comets which are observed today are likely separated by several generations of fragmentation events from their source comet (the comet of which they were a part on the preceding perihelion passage). This widespread and repeated fragmentation results in a nearly steady stream of arrivals which have very different orbital elements and in most cases appear unrelated to each other.

As of March 2009 there are more than 1400 known Kreutz comets. This includes 8–10 which were seen from the ground (and possibly another 20 or so if other poorly observed historical near-Sun comets are included), 19 which were seen with SMM and Solwind, 1358 which were discovered with SOHO, and 18 which were discovered with STEREO. The average elements of the SOHO and STEREO observed comets are q=0.0056±0.0013 AU (note that 1 $R_\odot$ = 0.0046524 AU, hence the term "sungrazing"), ω=79.7°±11.9°, Ω=0.4°±14.9°, and i=143.2°±3.9°. Due to short orbital arcs, the eccentricity is indistinguishable from 1.0 for all but the brightest few members seen from the ground, making the period of individual comets highly uncertain but believed to be between 500–1000 years. More than 90% of all Kreutz comets have orbits which resemble the "Subgroup I" orbit noted by Marsden (1967)

while the remainder have orbits closer to the "Subgroup II and IIa".

In this paper we reduce and analyze photometry of the Kreutz comets observed by SOHO from 1996–2005. In §2 we discuss SOHO/LASCO. We summarize the image calibration in §3 and the aperture photometry in §4. We present the lightcurves in §5 and interpret the photometry in §6. We discuss the population of the family based on the comets observed by SOHO in §7. Possible future observations are discussed in §8 and conclusions are given in §9.

2. Overview of SOHO/LASCO

NASA's SOlar and Heliospheric Observatory (SOHO) satellite was launched in December 1995 and began taking data in January 1996. It is in a halo orbit around the Earth-Sun Lagrange point L1. SOHO contains a suite of instruments designed to continuously observe the Sun and the near-solar environment at varying wavelengths. By far the most prolific instrument for observing comets has been LASCO, which has discovered more than 1500 comets since 1996 and has observed other comets including 2P/Encke and 96P/Machholz 1 (Biesecker et al. 2002; Grynko et al. 2004; Lamy et al. 2003). Up to date lists of all comets discovered by LASCO can be found on the "Sungrazing Comets" website maintained by NRL[6]. This paper deals with the comets observed by LASCO, which is explained in more detail below.

[6]http://sungrazer.nrl.navy.mil/.

2.1. LASCO

LASCO contains three coronagraphs, C1, C2, and C3, which have nested fields-of-view ranging from 1.1–30 $R_\odot$ on the plane of the sky. The innermost coronagraph, C1, has an annular field of view ranging from 1.1–3.0 $R_\odot$. It is internally occulted, and has a narrow passband Fabry-Perot interferometer tuned to hot coronal emission lines (Brueckner et al. 1995). C1 has not been used regularly since 1998 June 24, thus telemetry since then has been re-allocated to the C2 and C3 coronagraphs. No comets have been seen in C1, nor was it designed to observe them. Therefore, it is omitted from further discussion.

The outer two coronagraphs, C2 and C3 have annular fields of view from 2.0–6.0 $R_\odot$ and 3.7–30 $R_\odot$, respectively. C2 was deliberately designed to overlap both C1 and C3. Both C2 and C3 are externally occulted broadband imaging telescopes. Each telescope has a filter wheel, a polarizer wheel, a shutter, and a 1024×1024 pixel CCD. The pixel scale is 11.9 arcsec pixel^{-1} for C2 and 56 arcsec pixel^{-1} for C3 (Brueckner et al. 1995). The specifications for C1, C2, and C3 are summarized in Table 1.

[TABLE 1]

The synoptic programs utilize approximately 85% of the available daily telemetry[7]. Originally, the white light synoptic program obtained one image each from C1 and C2 every 30 minutes, and an image from C3 every hour, with most images having a reduced field of view (most frequently 1024×768). However, since late 1998, typically three full-resolution (1024×1024) C2 orange and two full-resolution C3 clear images are taken per hour. A polarization sequence using C2 and C3 is taken 1–2 times per day, and a color sequence is taken with C2 and C3 sporadically (sometimes as frequently as once per day, often as

[7]http://lasco-www.nrl.navy.mil/index.php?p=content/handbook/hndbk.

infrequently as once per week), usually at half resolution (2×2 pixels binned so the full image is 512×512).

2.2. SOHO Mission Interruptions

SOHO has operated nearly continuously since launching in late 1995. It suffered a major interruption from 1998 June 25 until 1998 October 22, when it lost pointing and went into an uncontrolled spin. Smaller unplanned interruptions have occurred intermittently, such as a 6 week interruption from December 1998 until February 1999. Pre-planned interruptions for routine maintenance, calibration, and satellite control have also occurred, and will continue to occur throughout the mission. Since the malfunction of the high-gain antenna in mid-2003, SOHO has needed to be rolled 180° every three months to keep the solar panels continuously pointing at the Sun. During these "keyhole" maneuvers which last approximately three weeks, some of the instruments are shut down. For a few days on either side of the roll maneuver, this frees up enough bandwidth and memory to increase the cadence of the C2 camera to five full resolution images per hour.

3. Calibrating Images

The SOHO/LASCO images we use for photometric reductions are "level-0.5" images which are publicly available via the SOHO website[8]. Level-0.5 images have been processed from the original data stream from the spacecraft (level-0) into fits files and oriented so that solar north is at the top of the image, however there is still a slight roll angle of each telescope from true solar north (typically much less than 1°). These images have units of DN (digital

[8]http://sohowww.nascom.nasa.gov/data/realtime-images.html.

number or counts).

Reductions were done in IDL using many of the Solarsoft IDL routines[9]. Beginning with a level-0.5 image we first subtract the offset bias. Next, we multiply the exposure time given in the FITS header by an exposure correction factor which is calculated for each image by the SOHO team (typically very close to 1.0) and divide the bias subtracted image by the true length of exposure to convert it to a flux (DN sec^{-1}). Then we multiply the bias subtracted, normalized image by the vignetting function[10]. The vignetting in C3 changed slightly due to a shift in the optics during the mission interrupt in 1998. Thus, three different vignetting functions are used when calibrating images: C2, C3 pre-interrupt, and C3 post-interrupt.

We construct a median background image from four images, two prior to the image of interest, and two after the image of interest, each processed to DN sec^{-1} as above. The images used in the background calculation are chosen to be as close in time to the image of interest as possible without contamination of the extracted region around the comet from either the comet, background stars, or anomalies such as cosmic rays or missing blocks of data (occasionally blocks of data are lost during downlinking from the spacecraft). We construct a background image using only images with the same telescope configuration (detector, filter, polarizer, summing on the chip, and telescope orientation). Occasionally fewer than four images are available for the background calculation, in which case the maximum number

[9]Solarsoft is a data reduction and analysis package for solar physics, notably SOHO. It can be downloaded at http://sohowww.nascom.nasa.gov/solarsoft/.

[10]This corrects for the reduction in light received at the CCD due to the optics of the telescope (namely the occulting disk and its support arm). The optical transmission varies radially, from zero at the center (behind the occulting disk) to nearly 1 at the edges. Superposed on this, the arm supporting the occulting disk (the "pylon") extends at a 45° angle from the southeast corner in unrolled images (the northwest corner in rolled images) to the center.

available is used. In general, images which were taken more than 24 hours apart are not used, as transient solar activity causes the background levels to vary substantially over these timescales. We create the background image by taking the median value at each pixel. We then subtract the background image from the processed image of interest yielding the final processed image which has units of DN $\sec^{-1}$.

Equations 1 and 2 summarize the processing:

$$processed\ image = \left(\frac{raw\ image - bias}{exposure\ time \times exposure\ factor}\right) \times vignetting \quad (1)$$

$$final\ image = processed\ image - median\ of\ neighboring\ processed\ images. \quad (2)$$

4. Aperture Photometry

We calculated aperture photometry from processed images created as described in Section 3 using IDL. We used the MPFIT2DPEAK routine[11] to calculate a circular gaussian and find the optocenter of the comet. In the rare cases where the centroid routine did not converge on the comet (typically due to a bright star or cosmic ray nearby) it was forced to the whole-pixel comet position as determined by eye. Using the center specified by the centroiding routine, we then used the APER routine[12] to calculate the fluxes inside circular apertures of varying radii. We selected the aperture size to encompass the coma while minimizing the contamination from stars and cosmic rays. For comparison across all comets,

[11]MPFIT2DPEAK is part of a library of IDL routines made publicly available by Craig Markwardt at http://cow.physics.wisc.edu/∼craigm/idl/mpfittut.html.

[12]APER is an IDL routine which calculates concentric aperture photometry. It is based on the IRAF routine DAOPHOT and is publicly available from the Goddard IDL Astronomy User's Library (http://idlastro.gsfc.nasa.gov/).

a circular aperture of radius 6 pixels (4.4 arcmin^2) was selected for C2 and 4 pixels (43.8 arcmin^2) was selected for C3[13].

4.1. Conversion to Visual Magnitudes

We converted the flux (DN sec^{-1}) to visual magnitude by

$$m = ZP - 2.5log(flux) \tag{3}$$

where m is the visual magnitude, ZP is the zero point conversions calculated by the SOHO team (Thernisien 2003; Llebaria et al. 2006), and flux is the aperture integrated flux in DN sec^{-1}. The zero points were calculated using hundreds of stars which pass through the field of view annually, and have changed slightly as the detector sensitivity has decreased over the life of the mission (by ∼0.4% per year in C3 and by ∼0.7% per year in C2 (Thernisien et al. 2006; Llebaria et al. 2006)). We use the global zero point calculated from 1996–2004 for C2 and from 1996–2003 for C3, and include an uncertainty due to the changing zero point of ±0.05 mag in the error estimate.

4.2. Normalization of the Magnitude

In order to compare the lightcurves of comets directly, it is necessary to correct for the effects of the changing geometry. Traditionally, comet magnitudes are normalized to r=Δ=1 AU using the equation

$$m_0 = m_1 - 2.5nlog(r) - 2.5klog(\Delta) - \Phi(\theta) \tag{4}$$

[13]These radii are for full resolution 1024×1024 images. Half resolution 512×512 images use apertures with half the radius.

where m_0 is the "absolute" magnitude normalized to r=Δ=1 AU, m_1 is the observed magnitude at the distances r and Δ, r is the heliocentric distance, n is the index of the brightening as a function of r, Δ is the geocentric distance (in this case Δ is the spacecraft distance), k is the index of the brightening as a function of Δ which is assumed to be 2, and $\Phi(\theta)$ is the phase dependent magnitude correction.

Since the focus of our study of the lightcurves is to derive the dependence of the brightness on the heliocentric distance, the apparent magnitude is corrected for Δ and phase angle, but not for r. Comet fluxes are corrected for Δ by normalizing to 1 AU from the spacecraft. SOHO is in a halo orbit around the Earth-Sun Lagrange point L1. The correction for Δ assumes that SOHO is always at L1 and does not correct for the minor deviations from L1 caused by its orbit. These deviations are less than 1% of the comet–spacecraft distance and their effect on the magnitude is much less than the uncertainty from the photometric reductions (discussed in Section 4.3). Therefore they have been ignored.

The correction for phase angle is much less straight forward and potentially has a much larger effect on the interpretations of the light curves. Phase angle, θ, is defined as the Sun-comet-observer angle. Most comets observed from the ground are at relatively modest phase angles and the geometry change during a series of observations is typically minimal. As a result, phase angle is often ignored for comets observed near 1 AU, and when included, the correction is typically a simple linear correction of 0.03–0.04 mag degree^{-1} (Jewitt 1991).

Due to their highly eccentric orbits, small perihelion distances, and high velocities, Kreutz comets observed close to perihelion can undergo dramatic changes in phase angle (up to 50°) over very short timescales (less than 2 days). Furthermore, many are seen at large phase angles, some in excess of 150°. Only a few non-sungrazing comets have been observed at large phase angles. These include 1P/Halley, Skjellerup-Maristany (1927 IX = 1927k = 1927 X1), West (1975 VI = 1975n = C/1975 V1), Bradfield (1980t = C/1980 Y1),

96P/Machholz 1 (in 2002), C/2004 F4 (Bradfield), and C/2006 P1 (McNaught), all of which showed large increases in brightness (Ney & Merrill 1976; Ney 1982; Marcus & Seargent 1986; Gehrz & Ney 1992; Grynko et al. 2004; Marcus 2007b,c). Thus, it is necessary to correct the apparent magnitudes for the changing phase angle before attempting to understand the heliocentric brightness dependence.

Kolokolova et al. (2004) combined observations of a number of comets over a wide range of phase angles and produced a plot (their Figure 1) for the phase dependence of cometary albedo due to scattering off of dust in the coma. This shows a strong forward-scattering (scattering off of dust in the coma in roughly the same direction that photons were traveling) surge at phase angles greater than 100°, a relatively flat region at intermediate phase angles, and a slight back-scattering (scattering off of dust in the coma in the direction opposite the initial direction of motion of the photons) peak at phase angles smaller than 30°.

Marcus (2007b) examined the phase dependence of coma brightness due to dust, deriving a "compound Henyey-Greenstein" (HG) model of the phase function which combines separate HG functions for forward- and backscattering. Similar in shape to the Kolokolova et al. (2004) figure, this model can be adjusted for varying coma dust-to-gas light ratios, and accurately predicted the surge in brightness of C/2006 P1 (McNaught) at large phase angle (Marcus 2007a,c). The full form of the compound HG model is given in Equation 1 of Marcus (2007c):

$$\phi(\theta) = \frac{\delta_{90}}{1+\delta_{90}} \left[k \left(\frac{1+g_f^2}{1+g_f^2-2g_f cos(180-\theta)} \right)^{\frac{3}{2}} + (1-k) \left(\frac{1+g_b^2}{1+g_b^2-2g_b cos(180-\theta)} \right)^{\frac{3}{2}} + \frac{1}{\delta_{90}} \right] \quad (5)$$

where $\phi(\theta)$ is the scattering function which can be converted to a magnitude by $\Phi(\theta)$=2.5log[$\phi(\theta)$], θ is the phase angle, δ_{90} is the dust-to-gas light ratio of the coma at $\theta = 90°$, k is the partitioning coefficient between forward- and back-scattering ($0 \leq k \leq 1$), and g_f and g_b are the

forward- and back-scattering asymmetry factors ($0 \leq g_f < 1$ and $-1 < g_b \leq 0$). Marcus (2007b) fit the data using g_f=0.9, g_b=–0.6, k=0.95, and δ_{90}=1 for a "usual" comet or δ_{90}=10 for a "dusty" comet. The function is normalized to 0 magnitude correction at a phase angle of 90°.

[FIGURE 1]

The scattering off dust is strongly dependent on the phase angle but the emission from gas in the coma is isotropic. As will be discussed in Section 5.3, Kreutz comets appear ∼1 magnitude brighter in the orange than in the clear filter, which is attributed to sodium emission. The contribution of the isotropic sodium emission to the flux must therefore be accounted for in order to properly apply the scattering correction. In Section 6, we estimate the flux of sodium emission necessary to cause the comets to appear ∼1 magnitude brighter in the orange than in the clear filter. The ratio of the flux due to the solar continuum (ie. scattering off the dust in the coma) to the flux due to the sodium emission (ie. gas) is δ_{90} = 0.52 for the C3 clear filter and δ_{90} = 0.16 for the C2 orange and C3 orange filters. These values of δ_{90} result in a smaller correction due to phase angle than was found by Marcus (2007b) for typical comets but are necessary to account for the strong contribution of sodium to the apparent brightness of the Kreutz comets. The other parameters were left unchanged, as they proved robust for the sample of six comets fit by Marcus (2007b,c). With these parameters, we use Equation 5 to correct the apparent visual magnitude to a phase angle of 90°. We plot the phase function for dust-to-gas ratios of 1, 0.52, and 0.16 in Figure 1.

4.3. Estimating the Error

The total error (in magnitudes) is a combination of the errors from the various components which went into the magnitude calculation added in quadrature. These include

uncertainty in the counts (calculated using counting statistics for the electrons received on the CCD), heliocentric distance (assumed to be 1%), phase angle (estimated to be 10% of the magnitude correction), and the zero point scale (estimated to be ∼0.05 mag to account for the decreasing sensitivity of the detectors). Other sources of uncertainty were ignored because they were much smaller than the above estimated errors. These include the bias, dark count, exposure time, vignetting function, and several other characteristics of the CCD and telescope optics which are discussed by Morrill et al. (2006).

5. Lightcurves

Prior to SOHO, most Kreutz comets had only been seen after perihelion (most ground observed comets) or inside of ∼15 $R_\odot$ (the SMM and Solwind comets). A surprising trait of the Kreutz comets observed by SOHO is the shape of their lightcurves, first discussed in Biesecker et al. (2002) and illustrated in Figure 2. Typical Kreutz comets brighten steadily as they approach the Sun, begin to flatten out at ∼16 $R_\odot$, reach a peak in brightness prior to perihelion at a distance of 10–14 $R_\odot$, then fade as they continue to approach the Sun. Occasionally the fading flattens out or they brighten again at distances inside of ∼8 $R_\odot$ before disappearing. No Kreutz comet observed by SOHO has ever been seen after perihelion. Due to the seasonal geometric effects (discussed in Section 7.2), data gaps, and/or the sensitivity of the detectors, most comets are not observed well enough to exhibit all of these features. However, nearly every comet displays some component of this general shape, and none are in contradiction to it.

[FIGURE 2]

In this section we discuss the lightcurves of the 924 comets which reached perihelion from January 1996–January 2006 for which we have calculated photometry. The photometry was

calculated as described in Sections 3 and 4, and has been normalized to unit SOHO-centric distance and corrected for phase angle unless otherwise noted.

5.1. Peak Distance and the "Universal Curves"

Biesecker et al. (2002) studied the first 141 Kreutz comets observed by SOHO from 1996–1998. Of these, 17 were determined to reach a peak brightness in C3 without saturating the detector (the peaks are not well observed in C2 so these were excluded). The peak distances of these 17 were found to be bimodal, with 11 comets reaching peak brightness at a slightly larger heliocentric distance than the remaining 6. When curves were fit to these groups, the 11 member Universal Curve 1 (UC1) peaked at 12.3 $R_\odot$ while the 6 member Universal Curve 2 (UC2) peaked at 11.2 $R_\odot$. Furthermore, UC2 brightened and faded more rapidly than did UC1. With our much larger sample size, we are equipped to more rigorously test the bimodality of peak distance and the existence of the universal curves.

We were able to determine a peak in the lightcurve for 79 of the 924 comets in our sample, 65 in C3 and 14 in C2. Peaks were determined by a combination of fitting a quadratic to the data and by selecting the single brightest photometric values. It is difficult to determine the exact peak distance of most light curves as they often have a broad, flat peak over a distance of 1–2 $R_\odot$. Thus we estimate the uncertainty in peak distance could be as large as 0.5 $R_\odot$. Six comets were observed to peak in C3 but saturated the detector so they have been omitted: SOHO-54 (C/1998 K10), 55 (C/1998 K11), 111 (C/2000 H2), 347 (C/2001 R2), 367 (C/2001 U9), and 614 (C/2003 K7)[14]. We omitted eight of the 17 comets which were included in the Biesecker et al. (2002) sample: SOHO-10 (C/1997 K1), 13 (C/1997 L4),

[14]We include SOHO numbers in this discussion for comparison with the nomenclature of Biesecker et al. (2002). These are simply the order in which the comets were discovered. IAU designations are used elsewhere.

17 (C/1996 H1), 22 (C/1996 O2), 23 (C/1996 O4), 29 (C/1997 R3), 30 (C/1997 S1), and 37 (C/1998 A1). These are among several dozen comets for which it is likely that the peaks were observed, however the data near the peak are sparse and/or noisy and we opted to exclude them. The distance and brightness of the lightcurve peak for these comets is given in Table 2. The photometry discussed in this paper is available through the Planetary Data System[15] and lightcurves will be submitted to the International Comet Quarterly[16].

A histogram of the heliocentric distance of peak brightness for the comets observed to peak in C3 is shown in Figure 3. The histogram has a maximum at 12.25 $R_\odot$ and a shoulder at 11.25 $R_\odot$. These features are consistent with the bimodality seen by Biesecker et al. (2002) (peaks at 11.2 and 12.3 $R_\odot$). However, unlike the Biesecker et al. (2002) sample, we see a broad range of peak distances from 10.5–14 $R_\odot$. Thus, while the sample retains the preference for peaking in brightness near 11 or 12 $R_\odot$, there is a continuum of peak distances centered around 12 $R_\odot$.

[FIGURE 3]

As mentioned previously, we omitted eight of the 17 comets in the Biesecker et al. (2002) sample because we could not confidently identify their peaks. Seven of these comets were in their UC1 (leaving only four UC1 comets) while one was in their UC2 (leaving five UC2 comets). Our best estimates of the distance of peak brightness for these eight comets range from 10.7 to 13.2 $R_\odot$. Inclusion of these eight comets in Figure 3 does not affect the conclusion of a continuum of peak distances. These eight comets represent nearly half of the Biesecker et al. (2002) sample, weakening the argument for bimodality. However, the remaining nine comets show an even larger bimodality of peak heliocentric distance: 12.8

[15]http://sbn.pds.nasa.gov/.

[16]http://www.cfa.harvard.edu/icq/icq.html.

$R_\odot$ for UC1 and 11.2 $R_\odot$ for UC2 using our data.

The geometry of the orbit makes it rare to see Kreutz comets at heliocentric distances larger than 10 $R_\odot$ in C2. Since we require there to be a clear trend of both brightening and fading around the peak, it becomes increasingly more difficult to observe a peak in C2 the larger the heliocentric distance of the peak. As a result, little can be inferred from the peak distances for the comets observed to peak in C2. The 14 comets observed to peak in C2 had peak distances between 10.6 and 11.9 $R_\odot$. The lack of observed peaks beyond 12 $R_\odot$ should not be considered real, but instead is a product of the viewing geometry.

The opposite effect may occur to a lesser extent in C3. While the C3 field of view extends to 3.7 $R_\odot$ in the plane of the sky, the photometry becomes increasingly unreliable at small distances as the vignetting and sky background increase and transient solar activity becomes more common. In principle comets should be observable until well after their peak in C3, however it is possible that some peaks are not recognizable due to the increasing difficulty of observing comets at small elongations. This is more likely to occur for fainter comets and comets which reach a peak at smaller heliocentric distances.

We next investigated whether the universal curves were evident in our larger sample. Rather than looking strictly at the distance of peak brightness, we considered the shape of each comet's lightcurve. Although we do not see a bimodality, there appears to be a correlation between the distance of peak brightness and the shape of the lightcurve, as discussed by Biesecker et al. (2002). To further examine the possible correlation, we put the individual lightcurves in one of three groups (Figure 4). The choice of three groups is somewhat arbitrary. In principal four or five groups could be identified, however the number of comets in each group would become problematic for statistics. We constructed composite curves for each group by offsetting all the comets in a given group to peak at the same magnitude (peak magnitude = 1) and taking the median magnitude of all the observations

in a given heliocentric distance range. The curves are plotted in Figure 5 and have been offset so they all peak at 12 $R_\odot$. To avoid confusion with the nomenclature of Biesecker et al. (2002), we designate these groups A–C from largest peak distance to smallest. Column 6 of Table 2 lists the group of each of the comets observed to peak in C3.

[TABLE 2]

[FIGURE 4]

[FIGURE 5]

Curve A is similar to UC1. It contains 31 comets with a median peak distance of 12.3 $R_\odot$. Curve B contains 16 comets with a median distance of 12.1 $R_\odot$. Curve C is similar to UC2, containing 18 comets with a median peak distance of 11.3 $R_\odot$. Shifting the three curves in magnitude and log(r) so that they overlap at their peak brightness, curve C brightens most steeply while curve A has the shallowest slope of brightening. At distances larger than $\sim$24 $R_\odot$, all three curves have similar slopes. The slopes of fading are harder to distinguish than the brightening due to fewer observations over a smaller region and generally noisier data, however curve A fades the most rapidly, followed by curve B, with curve C fading the most gradually.

We searched for trends that might correlate with the characteristic shape of these curves. There were no trends between orbital elements (q, Ω, ω, or i) or peak brightness and the curves. Furthermore, there are members of all three curves in both subgroups I and II (discussed in Marsden (1967)), suggesting that the lightcurve behavior is not dependent on the major fragment from which each comet is descended. The curves do not show a seasonal dependence, although the number of comets observed to peak in C3 (regardless of the curve to which they belong) shows a seasonal dependence consistent with the overall detection rate in C3 (see Section 7.2).

Interestingly, 15 of the 16 comets in curve B have been discovered since mid-2002 (Figure 6). Prior to 2003, nearly all the comets observed to peak in C3 were members of curves A or C, however since then all but five comets have been in curves A or B. It is possible that this is diagnostic of a varying composition of the swarm of Kreutz comets as a function of true anomaly in the orbit. That is, there may be some clustering of composition on the timescale of years, and the comets with composition causing them to brighten similarly to curve B only began reaching perihelion en masse in 2003.

An alternative explanation is that the increase in comets which brighten similarly to curve B is a result of improved detection circumstances for SOHO. As discussed in Section 7.1, there have been numerous changes to the way in which SOHO observes since 2000 (and particularly since mid-2003), resulting in more C3 images being taken per hour. This increased cadence makes it more likely that comets will be well observed and therefore easier to identify the peak in the lightcurve, the criteria for being included in this study. It is possible that the flux of comets identified as belonging to curve B has remained constant throughout the mission, however our ability to recognize them as such has improved. For this reason we hesitate to ascribe the increase in curve B comets to compositional differences as a function of position in the orbit.

[FIGURE 6]

5.2. Brightening and Fading

Due to the geometry of the Kreutz orbit and periodic gaps in the imaging sequences, most comets are only observed over a portion of the typical brighten-then-fade curve. While this limits the number of comets for which the distance of turnover can be determined, there are many more partial lightcurves available to give information about the brightening and

fading behavior. We considered slopes (slope = x where brightness $\sim r^{-x}$) over three ranges: brightening at heliocentric distances larger than 24 $R_\odot$, brightening from 24–16 $R_\odot$, and fading from 10–7 $R_\odot$. We considered two regions for the brightening slope because there appears to be a break in the slope for many comets between 20–27 $R_\odot$. We calculated fading slopes for both C2 orange and C3 clear images, however we only calculated brightening slopes for C3 clear images as no comets were observed in C2 beyond 16 $R_\odot$ and no comets were observed well enough in C3 orange to calculate a slope. We did not calculate any slopes between 10–16 $R_\odot$ because this is the region where lightcurves turn over. We also did not calculate any slopes at distances smaller than 7 $R_\odot$ because the data are sparse and noisy, however the few comets which were well observed in this region tend to show a second brightening or a flattening out. We calculated slopes for all comets with at least five images within the specified ranges which could be reasonably well fit by a power law. This frequently excluded the faintest comets (typically fainter than magnitude ∼7) where the uncertainty in the magnitude was comparable to the extent of the brightening or fading. Histograms of the brightening (left panel) and fading (right panel) are plotted in Figure 7.

[FIGURE 7]

We calculated the slope in log(brightness) versus log(r) beyond 24 $R_\odot$ for 67 comets, finding that they brightened with a median slope of 7.3 (with a semi-interquartile range[17], SIQR, of 2.0). 181 comets had calculable slopes from 24–16 $R_\odot$ with a median slope of 3.8 (SIQR=0.7). Among comets observed to fade from 10–7 $R_\odot$, 145 were observed in the C2 orange filter with a median slope of −5.5 (SIQR=1.2) and 11 were observed in the C3 clear filter with a median slope of −3.9 (SIQR=0.7).

[17]Semi-interquartile range is a measure of volatility. It is half the distance between the 25^{th} and 75^{th} percentiles.

The change in the slope of brightening which occurs around 24 $R_\odot$ is striking. While there is significant spread in the slopes beyond 24 $R_\odot$, the slope is unmistakably steeper than the slope from 24–16 $R_\odot$. The spread in slopes beyond 24 $R_\odot$ is likely due to fewer images, higher noise, and the distance of the break in the slope varying from comet to comet and not always occurring at 24 $R_\odot$. It is unlikely that the steeper slope is a product of poor photometry caused by faint comets because there are comparable numbers of equally faint observations in the 24–16 $R_\odot$ range without a corresponding tail of steep slopes. Assuming the change in slope is real, it may be tied to an ongoing physical process of the nucleus which is typically exhausted around 24 $R_\odot$. We will consider possible scenarios in Section 6.

It is interesting to note that the brightening and fading in the C3 clear filter appears to be symmetric inside of 24 $R_\odot$ with the caveat that the sample of C3 clear fading is very small (14 comets). Combined with the fact that the fading in the C2 orange filter is steeper than the brightening or fading in the C3 clear filter (inside of 24 $R_\odot$), this confirms the heliocentric color dependence discussed in the next section.

5.3. Orange – Clear Magnitude Difference

While the shapes of the lightcurves in the orange and clear filters tend to be similar, the comets generally appear brighter in the C2 and C3 orange filters than in the C3 clear filter. There are relatively few overlapping orange and clear observations due to the geometry (comets are rarely observed simultaneously in C2 and C3) and the scarcity of C3 orange images. Furthermore, those that do overlap tend to be noisy due to the proximity to the C3 occulter for comets observed simultaneously in C2 and C3 and the very faint magnitudes of most comets observed beyond 20 $R_\odot$. Only a handful of comets have more than three overlapping orange and clear images, making it difficult to draw conclusions from the color

behavior of individual comets. Instead, we consider the orange – clear magnitude difference in the aggregate.

Figure 8 shows the orange – clear magnitude difference as a function of heliocentric distance. Images that were brighter in the orange than in the clear are negative. Orange filter images with clear filter images taken both before and after were included. A cubic spline was fit to the clear filter images and the interpolated magnitudes were subtracted from the orange filter magnitudes. Saturated images were excluded. Error bars were calculated by adding the orange and clear errors in quadrature, and the clear errors were estimated as the weighted average of the two nearest clear error bars. All C3 orange filter images were half-resolution 512×512 images while all C3 clear and C2 orange filter images were full-resolution. C3 orange filter images were typically taken as part of a polarizer sequence (no polarizer, 0°, +60°, and −60°). We include only the C3 orange filter images without polarization.

While there is substantial scatter in Figure 8, the trend is for comets to brighten slightly (or remain constant) in the orange relative to the clear until a distance of 15–20 $R_\odot$, then fade in the orange relative to the clear interior to this. In general, the comets are brighter in the orange than the clear except for a handful of images taken at distances smaller than 8 $R_\odot$ and a dozen or so points when the comet was only marginally observed leaving C3 beyond 10 $R_\odot$. The anomalously low points beyond 10 $R_\odot$ are likely due to C3 clear magnitudes which were artificially inflated by an uneven removal of transient solar activity. A quadratic fit weighted by the error bars (red line) suggests the peak in the orange relative to the clear occurs at ∼19 $R_\odot$. (Biesecker et al. 2002) found a similar color dependence using only C3 orange and clear images for 11 comets observed from 1996–1998.

[FIGURE 8]

This orange – clear behavior is consistent with the observation that comets fade faster

in C2 orange images than in C3 clear images (Section 5.2). Furthermore, it is evident in the lightcurves of the few comets observed extensively in both orange and clear filters. Figure 9 shows two of the best observed comets. In the left panel (C/2001 U7 = SOHO-365) the orange – clear difference is largest when the comet is first visible in C2 (at $\sim$10.5 $R_\odot$) and decreases as the heliocentric distance decreases. In the right panel (C/2001 R2 = SOHO-347) the orange – clear difference peaks between 15–20 $R_\odot$ (note that both detectors were saturated from 10–15 $R_\odot$ making these magnitudes unreliable) and is slightly smaller at distances larger than 20 $R_\odot$ and smaller than 10 $R_\odot$.

[FIGURE 9]

5.4. Size Distribution

The observed magnitudes can be converted to an estimate of the size of the nucleus. We assume that the brightness is due entirely to the surface area of dust grains in the coma which are reflecting sunlight. For simplicity we assume the coma is made of spherical dust grains 1 μm in diamter having albedo 0.04 (the size distribution of dust in the ejecta relative to the ambient coma of 9P/Tempel 1 peaked at 1-μm in diameter (Lisse et al. 2006) and the albedo of the nucleus of 9P/Tempel 1 was 0.04 (A'Hearn et al. 2005)). We then determine the effective radius a sphere of these particles would have been if it disintegrated completely to produce the observed brightness of the comet. If we assume the nucleus has totally disrupted to produce the dust in the coma, we find sizes ranging from 2–50 meters in radius.

In this manner, we can estimate the size distribution of the Kreutz comets seen by SOHO. Ideally we wish to calculate the size at the peak in brightness. However, because our sample is small and the peak is generally only well determined for bright comets, the size distribution calculated from comets observed to peak is inconclusive (Figure 10, left

panel)[18]. Therefore, we approximate the size distribution by using all comets which were observed between 10–15 $R_\odot$ in the C3 clear filter (Figure 10, right panel). While this does not necessarily include the peak brightness for all comets, most are observed very close to peak, so the distribution should be close to but somewhat steeper than the true distribution. We do not include C3 orange filter observations because very few comets were observed in this filter and their inclusion would skew the results towards too many large comets since the comets are brighter in the orange filter, implying a larger nucleus. We do not include C2 observations because most are only observed inside 12 $R_\odot$ and many are too far past their peak brightness, skewing the results toward too many small comets. We fit a line to the data in log(number) vs. log(radius) space, with the slope being the power law exponent. This results in a cumulative size distribution $N(>R) \propto R^{-2.2}$ from 5–35 meters in radius. The turnover for sizes smaller than ∼5 meters is likely artificial due to incompleteness and the seasonal dependence of the limiting magnitude. The lack of comets larger than 30 meters may be real and indicative of a turnover in the distribution or it may simply be small number statistics.

[FIGURE 10]

5.5. The Effect of Normalizing the Photometry

As discussed in Section 4 we normalized fluxes to unit SOHO-centric distance and applied a correction for the phase angle. Since these corrections have a seasonal effect on the lightcurves, they alter individual lightcurves differently. The largest effect is generally to the intrinsic magnitude, as comets observed at very large phase angles (greater than 150°) can

[18]Here we included the six comets which saturated the detector for completeness. While their sizes may be slightly underestimated, their exclusion implies a misleadingly small upper end of the size distribution.

appear two or more magnitudes brighter than comets observed at intermediate phase angles (30–100°). This in turn affects the apparent size distribution of the family. The changing phase angle from image to image can also affect the shape of the lightcurve, altering the slope of brightening and fading and the distance of the peak of the lightcurve.

The first effect of the photometric normalization is on the distance of peak brightness. In Figure 11 we plot a histogram of the distances of peak brightness in C3 based on the raw magnitudes (left panel) and for the corrected magnitudes (right panel, replicated from Figure 3). In both cases the data peak at 12.25 $R_\odot$ and have a shoulder at 11.25 $R_\odot$, but the corrections spread the distribution out. Only 9 of the 65 comets reached a peak in brightness at a distance larger than 12.5 $R_\odot$ in the uncorrected sample, while 19 did in the corrected sample. The number of comets with peak distances smaller than 11.5 $R_\odot$ was unchanged. Thus, normalizing the photometry reveals that the distribution of peak distances is wider and less steeply peaked than would be inferred from the uncorrected sample.

[FIGURE 11]

The photometric normalization affects the shape of the lightcurve of some individual comets strongly. Figure 12 shows the uncorrected (black crosses) and corrected (all other points) lightcurves of C/2005 S1 (SOHO-1024). When first visible in C3, its phase angle was 98° resulting in a minimal change in magnitude. The phase angle steadily increased, reaching 128° when last visible in C3 and 143° when last visible in C2, resulting in increasingly larger corrections to the magnitude. As a result, after correcting for phase it appeared to brighten less steeply, fade more steeply, and reach a peak in brightness at a larger heliocentric distance.

[FIGURE 12]

While the effect of photometric normalization on individual lightcurves can be significant, the overall effect on lightcurve shapes is mitigated by the fact that there are roughly

equal numbers of comets made to appear brighter or fainter These effects are summarized in Table 3. The median peak distance is slightly larger and the spread in peak distances is greater. The slope of the brightening in C3 beyond 24 $R_\odot$ is somewhat more shallow. The slopes of the brightening from 24–16 $R_\odot$ and fading in C3 are nearly unchanged and still symmetric. The slope of fading in C2 becomes slightly steeper. The spreads in the slopes of brightening and fading are essentially unchanged.

[TABLE 3]

Since differing δ_{90} values were used for calibrating the clear (δ_{90}=0.52) and orange (δ_{90}=0.16) filter images, the orange – clear magnitude differences are affected even though they are interpolated from clear filter images at the same time (and thus phase angle) as the corresponding orange filter images. The change is equal to the difference between the δ_{90}=0.52 and δ_{90}=0.16 lines in Figure 1. For phase angles (θ) smaller than $\sim$100° the change is less than $\pm$0.1 magnitude. For θ>100° the correction is larger in the clear filter than the orange, hence the orange – clear color difference increases, with an increase of $\sim$0.5 magnitude for θ>130°. About half of the orange – clear points have a phase induced magnitude change less than than $\pm$0.1 magnitude, however, due to the asymmetry of the phase correction, the average correction to the orange – clear magnitude was $-$0.17 magnitude. Thus, as a result of the phase correction the orange – clear magnitude difference is larger than in the uncorrected data, meaning a larger fraction of the light is due to sodium than would be inferred from the uncorrected data.

The limiting magnitude of both C2 and C3 is approximately 8. In practice, C2 is more sensitive to comets in the range 7–8 magnitudes than C3 because of its smaller pixel scale and better signal to noise, making detections easier. As a result, the dataset is relatively complete for comets brighter than apparent magnitude 7 in C3 and apparent magnitude 8 in C2. The correction for Δ and phase (Figure 13) reveals that the distribution of intrinsic

magnitudes is not as clear cut. A significant number of comets intrinsically too faint to be seen by SOHO are made bright enough to be visible due to phase effects (the excess of comets at magnitudes fainter than 8 in the histograms with hatching at +45°). Roughly equal numbers of comets experience phase related brightening and fading, however due to the asymmetric effect of scattering (when corrected to a scattering angle of 90°), comets may appear ∼2 magnitudes brighter but only ∼0.1 magnitude fainter. Since the most a comet would appear fainter due to phase is ∼0.1 magnitude, the limiting magnitudes to which the distribution is complete are essentially unchanged, ∼8 in C2 and ∼7 in C3. The turnover in the distribution for magnitudes fainter than this is a combination of the sensitivity of the detectors and the effects of the phase angle. The substantial numbers of magnitude 9–10 comets despite the limited annual times when these comets are visible suggests that there are larger numbers of comets at fainter magnitudes.

[FIGURE 13]

Despite the significant changes to the magnitude distribution due to the phase correction, the slope of the size distribution is unchanged. For all comets seen in the C3 clear filter from 10–15 $R_\odot$, both the uncorrected and corrected datasets yield a slope of −2.22 for nuclei of radius 5–35 meters. For comets brighter than the completeness limit for C3 (magnitude 7 which corresponds to a 4.9 meter radius), the phase angle affects the same proportion of comets of all sizes.

6. Discussion

6.1. Orange - Clear Magnitude Difference

The comets appear brighter in the orange filter than the clear filter by about one magnitude. This difference must be due to emission in the orange bandpass which is much brighter

in proportion to the reflected solar continuum in the narrower orange bandpass than it is to the reflected solar continuum across the wider clear bandpass. The emission seen in Kreutz comets consists of the bands typically observed in comets at larger heliocentric distances (e.g. CN, C_2, etc...), ions not seen at larger distances, and elements seen in the spectra of sungrazers ([O I], Na I, K I, Ca II, Cr I, Mn I, Fe I, Ni I, Cu I, and CN were reported in Ikeya-Seki by Preston (1967) and Slaughter (1969)). Of the emission lines seen in Ikeya-Seki, only [O I] (6300 Å) and Na I (5890 and 5896 Å) fall within the orange filter bandpass (5400–6400 Å). Since sodium is much brighter than the forbidden oxygen line, it is the most likely source for the excess brightness in the orange filter relative to the clear filter.

To test this, we estimated the increase in the sodium line relative to the solar continuum required to cause the orange filter to increase by ∼1 magnitude relative to the clear filter. We calculated the flux due to the scattering of the solar continuum by dust in each detector/filter combination (C3 clear, C3 orange, C2 orange) by multiplying the solar flux at each wavelength[19] by the transmission of the filter at that wavelength[20] and the quantum efficiency of the detector at that wavelength[21]. We then simulated the flux of sodium emission by adding a rectangle of width 10 Å centered at 5895 Å (to encompass both sodium D-lines) and of a variable height. The apparent magnitude was ∼1 magnitude brighter in the orange filters relative to the clear filter for a height of sodium emission ∼600 times stronger than the solar continuum at 5895 Å. The integrated flux due to the sodium emission was ∼1.9 times more than the integrated flux due to the solar continuum in the clear filter and 6.4 times more in the orange filter.

---

[19]We used the 1985 Wehrli Standard Extraterrestrial Solar Irradiance Spectrum from http://rredc.nrel.gov/solar/spectra/am0/wehrli1985.new.html.

[20]http://lasco-www.nrl.navy.mil/index.php?p=content/filter/filter.

[21]http://lasco-www.nrl.navy.mil/content/tech/QE/c3_qe.txt.

To convert this to an estimated mass of sodium, we then estimated that the contribution from the sodium emission was 1.9/2.9 of the total flux received by SOHO from the comet in the C3 clear filter. Next we divided the total flux of the comet by the g-factor for sodium[22], and converted this to a mass of sodium. For a 5^{th} magnitude comet this yields a mass of ∼1000 kg. The photoionization lifetime of sodium at 12 $R_\odot$ is ∼9 minutes. Therefore a production rate of ∼2 kg s^{-1} is required to sustain the brightness. In this manner we integrated the sodium production for the lightcurve of C/2005 S1, which was observed in C3 from 31.2–7.6 $R_\odot$ over 33 hours and reached a peak magnitude of ∼4.5 at 14 $R_\odot$. During this time it produced 1.7×10^8 g of sodium. This is a large fraction of the estimated mass of C/2005 S1 (4×10^9 g using the estimated size and a density of 0.35 g cm^{-3}), however if the nucleus is a factor of two larger, the sodium would represent less than 1% of the mass. This begins to be plausible, but it may imply that our size estimates are too small.

It is likely that emission from other atoms or molecules besides sodium contributes to the overall brightness, however the ∼1 magnitude orange – clear difference indicates that emission in the orange filter bandpass is by far the dominant emission in the visible range. It is also possible that as yet unidentified refractory silicates are responsible for emission in the orange filter bandpass. While we cannot rule out this possibility, the observation of strong sodium emission at small heliocentric distances in Ikeya-Seki (Curtis & The Sacramento Peak Observatory Staff 1966; Evans & McKim Malville 1967; Preston 1967; Spinrad & Miner 1968; Slaughter 1969) and C/2006 P1 McNaught (Snodgrass et al. (2007) and Voulgaris private communication 2007) confirms that sodium emission should be extremely bright at

[22]The g-factor is the emission rate per molecule. We estimated it to be 5.5×10^{-11} erg s^{-1} $atom^{-1}$ at 1 AU from Figure 2 in Watanabe et al. (2003) and scaled it by r^{-2} to 12 $R_\odot$. Note that the radial velocity of a typical Kreutz comet at this distance is ∼230 km s^{-1}, which is well beyond the dip in the g-factor due to the Swings effect.

the distances observed by SOHO, and the estimated mass of sodium to produce this is plausible if our size estimates are somewhat too small. Therefore the contributions from other emission sources are likely small compared with sodium emission.

An alternative explanation of the orange – clear magnitude difference is improper photometric normalization. The photometric zero points were calculated using thousands of images of dozens of F, G, and K stars repeated annually over the life of the mission (Llebaria et al. (2006); Thernisien et al. (2006); Thernisien private communication 2003). We consider the zero points to be reliable and conclude that the orange – clear magnitude difference is a real effect diagnostic of differences in the flux from that of the solar continuum.

6.2. Size Distribution

The sizes of coronagraphically observed Kreutz comets have consistently been estimated to be a few meters to tens of meters. MacQueen & St. Cyr (1991) estimated the brightest SMM comets to be ∼16 meters in radius prior to the onset of sublimation. Ly-α fluxes recorded by UVCS have yielded estimates of the diameters of three comets at distances from 3–7 $R_\odot$: 6.7 meters for C/1996 Y1 at 6.8 $R_\odot$ (Raymond et al. 1998), 5.0–6.7 meters for C/2000 C6 at 6.36–5.71 $R_\odot$ (Uzzo et al. 2001), and 7.8 meters (with an unresolved 5.4 meter companion) for C/2001 C2 at 4.98 $R_\odot$ (Bemporad et al. 2005). Sekanina (2003) estimated initial diameters ranging from 17–200 meters by modeling 27 lightcurves with varying effective latent energies of erosion (analogous to sublimation heat). Iseli et al. (2002) used the fact that no Kreutz comets have been seen by SOHO after perihelion to derive an upper limit for the radius of 63 meters if it was composed entirely of water ice and destroyed by sublimation alone.

Despite a number of simplifying assumptions, our estimate of the size distribution,

ranging from 2–50 meters in radius (Section 5.4), is consistent with these values. Before proceeding with an estimate of the total mass of the system, we consider the validity of these assumptions. First, we assumed that the brightness is due entirely to the reflection of sunlight off dust grains in the coma. In actuality, the brightness is a combination of scattering and emission. The scattering component consists of scattering from the coma and the nucleus. A bare nucleus (i.e. no coma) 50 meters in radius should have an apparent magnitude of $\sim$18 at 12 $R_\odot$. Since the faintest comets observed are approximately magnitude 9, we can safely ignore scattering off the nucleus in comparison with scattering off the coma. We have shown above that in addition to the scattering off the dust in the coma, the brightness is due to emission, and the dominant emission is likely sodium. Sodium emission likely represents a substantial fraction of the brightness, and since our size estimate has assumed that all brightness comes from dust, our size estimates may be too large.

A second assumption is that the comet has disintegrated completely into dust at the distance of peak brightness (10–14 $R_\odot$). This is very likely not the case as UVCS observations indicate the presence of a nucleus in all three comets observed by it at distances inside 7 $R_\odot$, although the nuclei are believed to have fragmented or sublimated completely by $\sim$3 $R_\odot$ (Raymond et al. 1998; Uzzo et al. 2001; Bemporad et al. 2005). If the nucleus has not been completely destroyed at the distance of peak brightness, then the total size of the nucleus plus coma is larger than that inferred from the brightness.

Because so few comets are observed well enough to determine a peak in the lightcurve, we have calculated the size distribution using all comets seen between 10–15 $R_\odot$. Since these are all observed near their peak in brightness, the size distribution should be close to the true distribution. However, since most of these lightcurves are incomplete, any additional observations would only make the inferred sizes larger since observations fainter than the brightest observed magnitude would not be used. Thus, the sizes of many of the incompletely

observed comets may be somewhat larger than estimated here.

If we assume the comet is made entirely of water ice and scale the water production rate from 10^{18} molecules s^{-1} cm^{-2} at 1 AU by a factor of r^{-2}, a comet which is ∼50 meters in radius when it enters the SOHO field of view will decrease in radius by 16 cm $hour^{-1}$ at 30 $R_\odot$, 36 cm $hour^{-1}$ at 20 $R_\odot$, and 143 cm $hour^{-1}$ at 10 $R_\odot$ (assuming a density of 0.35 g cm^{-3}). If we further assume the comet has a rotation period of 1 day, a thermal inertia of 50 W K^{-1} m^{-2} $s^{0.5}$ (the upper limit for the thermal inertia of 9P/Tempel 1 (Groussin et al. 2007)), and heat capacity C_p=2.05 J g^{-1} K^{-1}, its skin depth would be ∼1 cm. Even if the heat capacity is lower and the rotation period longer, the skin depth would not be more than 3–5 cm for reasonable values. Thus, the rate of erosion in the SOHO field of view is much larger than the skin depth. As a result, no volatile depleted mantle can form and the erosion exposes fresh ices which were buried below the surface until very recently.

As an analog, we use the ejecta released by the Deep Impact experiment which excavated nearly pristine ice below the surface of 9P/Tempel 1, resulting in a size distribution that was smaller than the ambient pre-impact coma and rich in water ice (e.g. Sunshine et al. (2007); Knight et al. (2007); Schulz et al. (2006); Fernández et al. (2007)). Lisse et al. (2006) found that the Deep Impact ejecta were dominated by 0.1–10 μm particles, with a peak in the size distribution at 1 μm. Our size estimate assumed that the coma was optically thin and consisted of uniform spheres of diameter 1 μm and albedo 0.04. While acknowledging that modeling the coma with a distribution of particles of diameter 0.1–10 μm might improve the size estimate, the uncertainties inherent in this estimate make an overly specific particle size distribution superfluous. Equivalent nuclear radii constructed entirely from spheres of diameter 0.1 μm or 10 μm differ from the 1 μm equivalent nuclear radius by a factor ∼2–3 (smaller particles have a larger surface area to volume and result in a smaller equivalent nucleus and vice versa).

We used an albedo of 0.04, as is commonly assumed for comets. However, all previous albedo measurements have been at much larger heliocentric distances. The low albedo of comets is believed to be due to organics, but at the heliocentric distances observed by SOHO the organics likely sublimate very soon after being exposed to sunlight. Thus the albedo of the dust may be higher than the 0.04 assumed and the comet may be smaller than that inferred from our estimates.

Based on the uncertainties in all of the assumptions, we estimate that the nuclear sizes are likely good to within a factor of two. Thus the actual size range may be 1–100 meters in radius.

The size distribution exponent α=2.2 is similar to the slope of the Jupiter family comets which is 1.73–1.91 (Meech et al. 2004; Lamy et al. 2004; Weissman & Lowry 2003) or 2.65–2.7 (Fernández et al. 1999; Tancredi et al. 2006). After accounting for the effects of fragmentation and sublimation, Lowry et al. (2008) estimate that the primordial slope was 1.83–2.01. The two populations were produced by different mechanisms (splitting for the Kreutz comets versus collisions for the Jupiter family comets), but it is nonetheless interesting that the slopes are similar. If the comets were allowed to continue in their orbits instead of disintegrating on the subsequent perihelion passage, they would likely continue to fragment, steepening the slope of the size distribution. If it is assumed that the cometesimals which formed the original Kreutz progenitor have maintained their integrity (their internal strength is stronger than their connection to neighboring cometesimals), then continued fragmentation should cause the size distribution to reflect the true size distribution of the cometesimals where the Kreutz progenitor formed. The Weidenschilling (2004) two-dimensional model for the formation of comets predicts they are composed of components ranging in size up to $\sim$100 meters. Thus the size distribution seen in the Kreutz today may be close to the primordial distribution, and the discontinuity in the cumulative size distribution between the ground

observed and SOHO observed comets (discussed in the next section) is reflective of two distinct populations: large bodies composed of 1–100 meter components and the components themselves.

6.3. Total Mass

To estimate the total mass of the Kreutz system, we need to correct the size distribution for the comets which were unobserved due to data gaps. From 1996–2005, the collective duty cycle for C3 with the clear filter was 0.868. We do not need to correct for the seasonal effects because our size distribution was calculated using only the comets which were large enough to have been observed regardless of the geometry. Over 10 years, we observed 219 comets bigger than 5 meters. Assuming a continuous distribution of comets throughout the orbit, this represent 0.868 of the total observable. For an 800 year orbit, this yields ∼20,000 comets larger than 5 meters in radius in the orbit. The cumulative size distribution is

$$N(> R) \approx 869 \times R^{-2.2} \tag{6}$$

where N(>R) is the number of comets year^{-1} larger than radius R (in meters) which reach perihelion. Assuming the density is 0.35 g cm^{-3}, this converts to a cumulative mass distribution of

$$N(> m) \approx 2.1 \times 10^{7} m^{-0.73} \tag{7}$$

where N(>m) is the number of comets year^{-1} larger than mass m (in grams) which reach perihelion. Note that Equations 6 and 7 predict the true number of comets in the system, and are slightly larger than the actual number observed by SOHO due to gaps in the data.

Extending Equation 6 to radii larger than 3.6 meters (which correspond to comets $\sim 8^{th}$ magnitude or about the nominal limiting magnitude of C3), we should have observed 267 comets between 3.6–5 meters in radius from 1996–2005, but only saw 162. Even after

correcting for the duty cycle, ∼30% of the expected comets in this range were unobserved. This is largely due to the viewing geometry, but is also due to the limited amount of time over which comets attain their peak brightness. A comet is required to be in at least 5 images to be confirmed by the SOHO team[23]. An average of 2–3 C3 clear images are taken per hour. Thus the comet must be above the minimum threshold for ∼2 hours to be discoverable. Near the lightcurve peak, the comet will travel ∼2 $R_\odot$ in 2 hours. So, for comets near the limiting magnitude, if the brightness peaks steeply the comet will not be detected, but if it has a broad peak it may be detected. Many of the faintest detections appear this way–they have no discernible slope, just 5 or so points barely above the limiting magnitude.

There are also fewer comets larger than 30 meters than expected. From the size distribution, we would expect 4.6 such comets in 10 years and two were seen. We tested the likelihood that the comets larger than 30 meters are from the same distribution as those smaller than 30 meters by assuming that an average of 0.00126 comets bigger than 30 meters arrives on a give day (4.6 comets in 10 years). We then generated a random number for each day for 10 years to determine whether or not a comet arrived on that day. This was repeated 10,000 times, yielding an average of 4.6±2.1 comets in the 10 year interval. 16.2% of the time the simulation resulted in 2 or fewer comets 30 meters or larger arriving in 10 years. Thus, there is about a 1 in 6 chance that the two comets larger than 30 meters seen from 1996–2005 were from the same size distribution as the rest of the SOHO comets. Until the baseline of observations is increased, we cannot conclude that there are signicantly fewer comets larger than 30 meters, and hence a break in the power law around 30 meters.

Sekanina (2002b) compiled observations of the ground observed Kreutz comets and calculated their lightcurve parameters. Only Ikeya-Seki was observed at r<50 $R_\odot$ (except

[23]Occasionally comets with fewer than 5 images have been confirmed. All of these clearly show cometary activity and were only in fewer than 5 images because the rate of C2 images was low.

for a single observation of the Great Comet of 1843 = 1843 I= C/1843 D1), however, we can extrapolate each comet's brightness using the lightcurve parameters. Setting r=12 $R_\odot$ and Δ=1 AU for each ground observed comet, we can compare the brightness at the distance of lightcurve peak for the SOHO observed sungrazers[24]. If we then make a crude assumption that the brightness is proportional to the square of the radius, we can derive an estimate for the nuclear size. Setting the size of an 8^{th} magnitude comet at 4 meters in radius (for Δ=1 AU, r=12 $R_\odot$), we estimate the nuclear radii as follows: the Great Comet of 1843 (1843 I = 1843 D1)≈8 km, the Great Southern Comet (1880 I = C/1880 C1)≈1.1 km, the Great Comet of 1882 (1882 II = 1882 R1)≈30 km, du Toit (1945 VII = C/1945 X1)≈0.6 km, Pereyra (1963 V = C/1963 R1)≈14 km, Ikeya-Seki≈4.3 km, and White-Ortiz-Bolelli (1970 VI = C/1970 K1)≈1.1 km. No nuclear condensation was seen for the Great Southern Comet of 1887 (1887 I = C/1887 B1). Sekanina (2002b) believed it to be much smaller, calling it a "transition object" between the bright ground observed ones and the faint SOHO observed ones, and Sekanina (2003) estimated its initial radius at ∼500 meters.

Assuming the distribution of comets seen by SOHO is constant throughout an 800 year orbit and setting N(>R)=1, we would expect the largest comet to have a radius of ∼500 meters. Thus, C/1887 R1 was likely the largest fragment in the distribution, and C/1945 X1 is consistent with the distribution if it is the largest comet in the orbit (we expect ∼0.3 comets 800 meters and larger). The size distribution cannot explain the six comets larger than 1.1 km, as we would expect ∼0.1 such comets in 800 years. We simulated this as above,

[24]The magnitudes for the 19^{th} century comets are generally for the nuclear condensation, while for the 20^{th} century comets, integrated magnitudes are given. The SOHO photometry uses a fixed aperture which more closely resembles the nuclear condensation. The integrated magnitudes imply brighter comets than the nuclear condensation, but for this order of magnitude calculation it is sufficient to assume they are equivalent.

assuming the size distribution holds at all sizes and the baseline over which comets bigger than 1 km have reliably been detected is 200 years. None of our 1000 simulations had more than 1 comet arrive during 200 years[25]. Even if our rough estimates of the nuclear sizes are an order of magnitude too large, we are still left with 3–4 comets larger than than the expected maximum size. Thus we conclude that there is a break in the size distribution which occurs by 500–1000 meters in radius (and possibly as small as 30 meters) and that the fragmentation of the Kreutz progenitor was relatively recent. With enough time, repeated splitting should cause the entire population to be described by a continuous power law. Alternatively, the distribution may not be uniform around the orbit, and the distribution seen by SOHO may not be representative of the distribution at other times.

Integrating over the size range 5–500 meters we find a total mass of the system of $\sim 4\times10^{14}$ g for a bulk density of 0.35 g cm^{-3}. We note that Sekanina (2003) found a more shallow size distribution and estimated the total mass to be $\sim 1\times10^{16}$–8×10^{17} g using only the photometry of the 26 brightest comets published by Biesecker et al. (2002). A total mass of $\sim 4\times10^{14}$ g is equivalent to a sphere of radius $\sim$650 m for a density 0.35 g cm^{-3}. The total mass is dependent on the upper cutoff of the size distribution. If the maximum size is $\sim$50 meters (the largest comet observed so far by SOHO), the total mass in the system is $\sim 5\times10^{13}$ g, corresponding to a sphere of radius $\sim$325 meters. Sekanina (2002b) concluded that C/1882 R1 was the largest Kreutz comet, estimating its effective mass at $\sim 10^{19}$ g. By extension from the sizes estimated from the lightcurves above, the masses of the six other most massive fragments range from $\sim 10^{15}$–10^{18} g. Therefore, the inferred total mass of the population of coronagraphically observed fragments is much smaller than the mass of any of

[25]If the near sun comets observed since the 16^{th} century and considered as possible Kreutz comets by Sekanina & Chodas (2007) are included, 23 additional massive comets are in the group and the size distribution fails miserably for large comets.

the bright-ground observed comets. This is further evidence that the splitting of the group was recent.

6.4. Rate of Brightening

Of the ground-observed Kreutz comets, only Ikeya-Seki was well observed prior to perihelion, while five were observed after perihelion: C/1843 D1, C/1882 R1, C/1963 R1, C/1965 S1, and C/1970 K1 (Sekanina (2002b) and references therein). The fading rate for the ground observed Kreutz comets was between $r^{-3.2}$ and $r^{-4.5}$, which is similar to the brightening rate we derived from 16–24 $R_\odot$ for the comets observed by SOHO ($\propto r^{-3.8\pm0.7}$). Despite being observed at much larger heliocentric distances, the brightness behavior of the largest comets (all of which survived perihelion) is remarkably consistent with that of the smallest. From this we conclude that the brightening seen in the SOHO field of view from 16–24 $R_\odot$ is due to the typical processes which cause the Kreutz comets to brighten rather than processes which are unique to the smallest comets, such as catastrophic disruption and subsequent disintegration.

The SOHO-observed Kreutz comets brighten $\propto r^{-7.3\pm2.0}$ beyond $\sim$24 $R_\odot$. Ikeya-Seki brightened near at a rate near r^{-4} from 1.02–0.03 AU (Sekanina (2002b) and references therein). Unfortunately, it was not observed from 50–20 $R_\odot$ prior to perihelion. After perihelion there were nine observations from 9–50 $R_\odot$, including three between 20–40 $R_\odot$. The lightcurve fluctuates about the r^{-4} line, but there is no obvious section which fades significantly steeper than this. If Ikeya-Seki experienced a significant period of brightening near $\sim r^{-7}$, it only occurred prior to perihelion and only from 50–20 $R_\odot$. Thus we cannot determine when the $\propto r^{-7.3}$ brightening begins, but conclude it is unlikely to extend beyond 50 $R_\odot$.

Sekanina (2000b) examined the tail morphology of nine Kreutz comets observed from 1996–1998, finding that the production of dust peaked at 20–30 $R_\odot$ and had $\beta \leq 0.6$ (β is the ratio of the force due to solar radiation pressure and the force due to the Sun's gravity). The distances of peak production correspond to the approximate locations of the changes in slope from $\propto r^{-7.3}$ to $\propto r^{-3.8}$. We compared the lightcurves of the 9 comets in the Sekanina (2000b) study with their inferred distance of peak dust production. While 8 of the 9 comets in the sample exhibited a change of slope between 20–30 $R_\odot$, the distances did not correlate well. Four transitioned at a larger distance than the inferred peak production distance, three approximately agreed, one transitioned at a smaller distance, and one showed no change in slope (this comet was anomalous in the sample; Sekanina (2000b) inferred its dust production peaked at 230 $R_\odot$).

66 comets in our sample were observed well enough to calculate a slope beyond 24 $R_\odot$. The vast majority of these had well defined tails as is common for bright comets observed by SOHO. The exceptions were all faint, making it difficult to determine the presence of tails, but in general these comets also had less obvious changes in slope at 20–30 $R_\odot$. While a more thorough investigation of the tail parameters is beyond the scope of the current work, it is likely that the tail formation is a result of the same process which causes the comet to brighten steeply, and warrants further study.

We suggest that the steep rate of brightening (and apparently the accompanying tail formation event) is due to the onset of activity of a previously inactive species (presumably a refractory organic) which results in an explosive outburst. In this scenario, the increasing insolation causes a buildup of pressure below the surface. At some point (the exact distance varying from comet to comet) the pressure exceeds the strength of the regolith and an outburst blows off much of the outer layer. The destruction of the regolith would deposit a large amount of small silicate dust grains into the coma, and the surface area of the coma

would continue to increase for some time while the ejected dust fragmented further. As the process slows, the comet returns to its $\propto r^{-3.8}$ brightening, offset brighter if the active surface area has increased as a result of the outburst. Alternatively, the onset of activity may trigger the entire nucleus to become active rather than just a few regions. In either case, the steeper rate of brightening ($\propto r^{-7.3}$) can be seen as a δ-function superposed on top of the $\propto r^{-3.8}$ rate. The increased surface area will result in the $\propto r^{-3.8}$ rate resuming at an elevated level after the initial burst fades. This is illustrated in Figure 14.

[FIGURE 14]

To test the rate of brightening beyond the SOHO field of view, we surveyed regions of the sky statistically likely to contain Kreutz comets approximately 3–6 months prior to perihelion using the MOSAIC camera on the KPNO 4-m telescope. We searched the images by aligning three consecutive images and blinking them to look for moving objects. Later, as comets were discovered by SOHO which should have been in the field of view, we searched the images again to look for comets near the expected positions. While as many as 12 comets may have been in the field of view, none were found, suggesting that they either brightened at a rate steeper than $\propto r^{-3.5}$ or that the orbital element uncertainties are larger than we had estimated. Additional fields at a different epoch provided by Scott Sheppard and Chad Trujillo from the Magellan 6.5-m telescope at Las Campanas also did not reveal any comets.

6.5. Qualitative Explanation of the Lightcurve

Previous interpretations of the lightcurves of the Kreutz group have focused on the apparent bimodality of the peak in brightness noted by Biesecker et al. (2002). Sekanina (2003) has explained the differences as corresponding to comets having differing latent energies of erosion and in some cases additional fragments too small or too recently separated to

be individually resolved. Kimura et al. (2002) attribute the two peaks as corresponding to fluffy aggregates of crystalline olivine (the peak at 11.2 $R_\odot$) and fluffy aggregates of amorphous olivine (the peak at 12.3 $R_\odot$). They further argue that the observed lightcurves are a superposition of two lightcurves: one due to olivine which peaks from 10–13 $R_\odot$ and one due to pyroxene which peaks inside 7 $R_\odot$, with the relative heights of the peaks at $\sim$12 $R_\odot$ and inside of 7 $R_\odot$ indicative of the abundance ratio of olivine to pyroxene.

Our photometric analysis shows that the distance of peak brightness is not bimodal, but is more nearly a gaussian centered at 12 $R_\odot$ and ranging from 10–14 $R_\odot$. Without the need to explain two distinct lightcurves, this can now be viewed as reflecting a spectrum of comets with similar compositions which behave slightly differently due to their unique fragmentation history, topography, rotation, etc... Rather than being confined to two narrow ranges, the peak distances actually vary over a fairly large region, representing a change of $\sim$30% in heliocentric distance between the largest and smallest peak distances.

We demonstrated that rather than the two "universal curves" which were discriminated by distance of the peak, the lightcurves have a continuum of shapes. To illustrate this, we arranged them into three groups (A–C) based on their shapes of brightening and fading. Group A had the most gradual slope of brightening and fading and the largest peak heliocentric distance. Group B had intermediate slopes of brightening and fading and peak distance. Group C had the steepest slope of brightening and fading and the smallest peak distance. These features can be explained by a continuum of compositions between amorphous and crystalline olivines. Kimura et al. (2002) showed that amorphous olivines sublimate more slowly and at larger distances than crystalline olivines. Thus the comets in group A have higher ratios of amorphous olivines to crystalline olivines than the comets in group B, which in turn have higher ratios than group C.

There does not appear to be a correlation between size of the nucleus and the distance of

peak brightness. We would expect a size dependence since bigger comets take longer to erode and therefore survive to a smaller heliocentric distance. However, as shown in Figure 15, if the erosion is dominated by water production, nuclei of nearly all sizes will survive until heliocentric distances smaller than the lightcurve peak at 10–14 $R_\odot$. The smallest nuclei will erode prior to the peak distances, but these are below the threshold for detection and therefore do not appear in our database. Since the distance of the lightcurve turnover does not correlate with the size estimate, the destruction of the nucleus by erosion is not the primary cause of the lightcurve turnover.

[FIGURE 15]

As explored by previous authors (e.g. Biesecker et al. (2002); Kimura et al. (2002)), the lightcurve shape is an amalgamation of numerous processes which depend on the heliocentric distance. These include but are not limited to the production of water and other volatiles from the nucleus, emission of sodium and other heavy elements, the sublimation of olivine, pyroxene, and other silicates from the coma and the nucleus, the photoionization lifetimes of particles in the coma, fragmentation, and tidal forces on the nucleus. Undoubtedly the unique evolutionary history of each comet contributes to its distinct shape, but we can explain the general shape as follows.

At large heliocentric distances, the comets behave like dynamically young comets, rich in ices and with a small dust size distribution due to frequent fragmentation exposing new surfaces, e.g. Sekanina (2000a, 2002a). Beyond 50 $R_\odot$ they likely brighten at a rate near $\propto r^{-4}$ as Ikeya-Seki did (Sekanina 2002b). Although it is unclear exactly where, at some point prior to entering the SOHO field of view most begin to brighten steeply, near $\propto r^{-7.3}$. This continues until $\sim$24 $R_\odot$ when the rate rapidly transitions to $\propto r^{-3.8}$.

Around 16 $R_\odot$ the lightcurve begins to turn over, reaching a peak between 10–14 $R_\odot$.

The turnover in the lightcurve is likely due to the rate of sublimation of dust grains in the coma exceeding the production rate of dust from the nucleus. Kimura et al. (2002) showed that sublimation of fluffy aggregates of amorphous and crystalline olivine occurs at 10–13 $R_\odot$. This will rapidly deplete the reflecting area of the coma. While the production rate (per cm^2) is increasing $\propto r^{-2}$, at some point the surface area of the nucleus becomes too small and the total production drops. The combination of a declining production rate and an increasing sublimation rate cause the lightcurve to turn over and fade rapidly. As shown in Figure 15, comets made entirely of water ice with initial radii from 20–50 meters prior to entering the SOHO field of view will be roughly 5–35 meters in radius at 12 $R_\odot$ (the size range of the SOHO observed comets), and will disappear entirely between 3–9 $R_\odot$.

Inside of $\sim$7 $R_\odot$, the comet will erode very rapidly. UVCS observations of three comets suggest that the nuclei disappear entirely by $\sim$3 $R_\odot$ (Raymond et al. 1998; Uzzo et al. 2001; Bemporad et al. 2005). Kimura et al. (2002) predict that the sublimation of crystalline and amorphous pyroxenes would cause a second peak at 4–6 $R_\odot$. The lightcurve data in this region are sparse, but are in general agreement with this as the lightcurves tend to level off or brighten again inside $\sim$7 $R_\odot$. An alternative explanation for this phenomenon is that fragments too small to be individually resolved and which have substantially higher erosion energies reach a peak in brightness in this region (Sekanina 2003). Since the range of peak distances indicates that the comets are relatively homogeneous, we find it unlikely that they would fragment into pieces with such disparate energies of erosion. Therefore we favor the final disruption of the nucleus and sublimation of pyroxene as the mechanism to cause this final brightening.

6.6. Lightcurve Behavior for the Comets Beyond the Sizes Seen By SOHO

The scenario described above should hold true for comets in the size distribution observed by SOHO. Comets with initial radii smaller than a few meters would be destroyed by erosion at larger distances than 10–14 $R_\odot$. These comets would never achieve the brightness necessary to be observed by SOHO, however if the size distribution holds, they should be numerous. While the nucleus of such a comet would have disrupted, the dust should continue along the orbit subject to the effects of radiation pressure. Thompson (2009) showed that the tail of comet C/2007 L3 consisted of particles emitted between 18 and 24 hours before perihelion (18–22 $R_\odot$) and which persisted until several hours after perihelion. Similarly, the tail of C/1979 Q1 was evident for 100 minutes after perihelion in Solwind images (Michels et al. 1982), and we have noted the phenomenon in a number of bright SOHO comets. Future coronagraphic missions with much greater sensitivity might observe the tails of comets too small for the nucleus to have survived into the SOHO field of view as headless comets.

Iseli et al. (2002) estimated that comets larger than 63 meters in radius would survive long enough past perihelion to be observed for some time by SOHO if they were composed entirely of water ice. Using an argument based on the energy of erosion, (Sekanina 2003) estimated that a comet would need to be 250–350 meters in radius for a small fraction to survive perihelion, and ∼500 meters in radius to survive until the subsequent perihelion passage. The largest comet in our sample was below either of these estimates, and was not seen after perihelion. The lightcurve of a comet which survives past perihelion should brighten more steeply when it reaches distances where its refractory grains begin to sublime. Based on the interpretation of the features of the SOHO observed comet lightcurves, we would expect the brightening to become more steep near 10–14 $R_\odot$ and 4–6 $R_\odot$ due to the sublimation of olivine and pyroxene, respectively, however we would not expect it to peak in brightness until perihelion. The lightcurve would be roughly symmetric about perihelion,

however it would disappear rapidly once the nucleus eroded away. It is possible that C/1887 B1 was such an object, being large enough to survive perihelion, but having no nucleus (or one so small that it was not outgassing appreciably), therefore appearing as a headless tail when first observed 0.46 AU after perihelion.

At least six comets large enough to survive perihelion and return (∼500 meters as estimated by Sekanina (2003)) have been seen (C/1843 D1, C/1880 C1, C/1882 R1, C/1963 R1, C/1965 S1, C/1970 K1), although the only one observed both before and after perihelion was C/1965 S1 Ikeya-Seki, whose lightcurve is plotted in Figure 1 of Sekanina (2002b). Its pre- and post-perihelion lightcurves are nearly identical in slope. Interestingly, the point at ∼12 $R_\odot$ prior to perihelion is ∼0.5 magnitude brighter than the next point interior to it at ∼11 $R_\odot$, and the slope inside of ∼13 $R_\odot$ is steeper than the slope for the whole range of observations (0.03–1.63 AU). With the exception of the brief fading between 11–12 $R_\odot$, Ikeya-Seki continued to brighten until perihelion. The bright point at 12 $R_\odot$ is consistent with the rapid sublimation of the olivine in the coma and the continuing steeper slope interior to that is consistent with the sublimation of olivine from newly released dust. There is a corresponding bright point at ∼12 $R_\odot$ in the post-perihelion lightcurve which is difficult to explain since we would not expect an increase in sublimation as the distance was increasing. Furthermore, the only point prior to it is slightly fainter than predicted from the average slope. While the lightcurves of the comets observed to survive perihelion demonstrate that the activity of Kreutz comets is nearly symmetric about perihelion, they were not observed well enough at small heliocentric distances to conclusively support or refute the particulars of the composition inferred from the coronagraphic lightcurves.

7. Population

7.1. Yearly Detection Rate

Over SOHO's first twelve years, 1996–2007, 1219 Kreutz family comets were discovered in its images (Table 4). The discovery rate has increased throughout the mission due to a number of factors. First, the telemetry bandwidth allocated to C2 and C3 increased from 1996 to 2000, resulting in more full resolution images per day. While an average of only 6 full resolution images were taken per day by both C2 and C3 in 1996, the rate had increased to about 60 per day in C2 and 40 per day in C3 by 2000, and has remained relatively constant ever since.

[TABLE 4]

The duty cycle, or the fraction of time SOHO takes images, also increased from 1996–2000. Following the definition of Biesecker et al. (2002), we define a gap in excess of four hours between full resolution images in a given telescope to be significant, with the time exceeding four hours considered to be lost time. All of the excess time is then summed for a whole year, divided by the total hours in a year, and subtracted from 1. A year with no missed time would have a duty cycle of 1.0 while a year with no full-resolution images would be defined to have a duty cycle of 0. Due to the lower bandwidth allocated to C2 and C3 as well as several significant hardware failures endured by the spacecraft, the duty cycle for both C2 and C3 from 1996–1999 only exceeded 0.80 once and was as low as 0.60. Since 2000 however, the yearly duty cycle in both telescopes has remained above 0.88. The average combined C2 and C3 duty cycle by year is given in column 7 of Table 6.

The "Sungrazing Comets" website became commonly used as a means of reporting

comet discoveries in late 2000[26]. This site allows amateur comet hunters to download images in near real time in several formats to search for new comets. Since mid-2000 nearly every Kreutz comet has been discovered in near real time. In addition to searching the real time images, many users have systematically combed the archives for earlier comets, and it is believed that very few Kreutz comets have escaped detection.

Beginning in mid-2003, SOHO has been rolled by 180° approximately every three months due to the malfunction of the high-gain antenna (discussed in Section 2.2). The roll periods cause an increase in detections in C3 due to the rotation of the occulting arm out of the path of Kreutz comets. This allows fainter comets to be discovered during the roll periods than would be seen if they arrived when the telescope was not rolled (discussed further in Section 7.2 below). Furthermore, there is an increase in the telemetry devoted to C2 for a few days on either side of each roll maneuver which causes a slight increase in the C2 detection rate by allowing fainter comets to be discovered (since they only have to remain above the threshold for a shorter amount of time to be detected). Taking all of the above factors into account, the period from 2004–2007 has the most complete temporal coverage and the most uniform month-to-month selection effects. Thus we consider this time frame to be representative of the true detection rate of SOHO.

7.2. Seasonal Variability

There is a distinct seasonal variation in the observation rates of Kreutz comets (Figure 16). Observations of comets in C2 (these comets may or may not be seen in C3) peak strongly from April to June and again from October to December each year, while C3 ob-

[26]Publicly available reporting of amateur discoveries began in late 2000 however the SOHO team had been working privately with amateurs for several years prior to this.

servation rates (these comets may or may not be observed in C2) are more constant, but dip strongly in April and weakly from March to June and November to December. Since many comets are seen in both C2 and C3 and since C2 is more prolific than C3, the combined discovery rate is relatively flat with peaks that mirror the peaks in C2. This seasonal variability is due to the combination of two factors: the geometry of the Sun-SOHO-Kreutz system and the brightness behavior of Kreutz comets at small heliocentric distances. We discuss these effects below.

[FIGURE 16]

7.2.1. Obstruction By the Occulting Arm

Kreutz comets approach the Sun from the south (the bottom of unrolled SOHO images when north is up and east is to the left). Figure 17 shows the track of a typical Kreutz comet through the SOHO field of view on the 15^{th} of each month. From January through May, they approach from the bottom left. In June the track begins to pass to the other side of the field of view and comets move nearly straight up from the bottom middle. From July through November they move diagonally up from the bottom right. Finally in December the track begins to swing back to the left and comets move nearly straight up from the bottom middle.

[FIGURE 17]

The occulting arms on C2 and C3 extend from the bottom left corner to the middle at roughly a 45° angle in unrolled images and from the top right in rolled images. Thus, comets which arrive from January to early May frequently cross the occulting arm in unrolled images. This reduces the counts recorded, sometimes completely obscuring the comet and preventing detections. This has a minimal effect in C2, but is strong in C3 where the vignetting is more

severe, and results in a lower discovery rate during these months.

This effect has been mitigated since mid-2003 by the 180° rolls necessary every ∼3 months since the malfunction of the high-gain antenna. When the telescope is rolled, the occulting arm extends from the northwest and does not cross the Kreutz track. This has improved the discovery rate during times when the track is usually obstructed by the occulting arm. These include: 2003 December 31–2004 March 29, 2004 December 23–2005 March 21, 2005 December 16–2006 March 13, and 2006 December 6–2007 March 5. This effect can be seen in the C3 discoveries in January to April in Figure 16. During this time, SOHO has always been rolled in January and February, has been rolled about half the time in March, and has never been rolled in April. The discoveries in C3 mimic this pattern: 33 comets were observed in C3 in January, 33 in February, 22 in March, and only 6 in April.

7.2.2. Elongation of Peak Brightness

A second effect of the geometry is on the elongation at which the Kreutz comets reach peak brightness. The SOHO-Sun line is approximately in the plane of the Kreutz orbit from April to June and October to December. During these months, comets approach the Sun from behind (April to June) or in front (October to December) and reach their peak brightness at a smaller solar elongation. During these months, typical Kreutz comets are at a heliocentric distance of 8.5–12 $R_\odot$ when they enter the C2 field of view, making them visible in C2 at or soon after their peak brightness. From January to March and July to September, the SOHO-Sun line is roughly perpendicular to the plane of the Kreutz orbit. During these months, typical Kreutz comets are at a heliocentric distance of 6–7 $R_\odot$ when they enter the C2 field of view. Thus, they do not appear in C2 until well after peak brightness, and fewer comets are visible. The heliocentric distance at which comets leave C2 has no effect

on discovery rates, as only the very brightest comets are still seen leaving C2.

This plane-of-sky geometry has a small but opposite effect on comet detections in C3. The maximum heliocentric distance at which comets leave C3 varies from 3.5–8.5 $R_{\odot}$ throughout the year, meaning the peak brightness is always within the C3 field of view. However, the signal to noise and vignetting are worse closer to the occulting disk, so there is a preference for geometries in which the comet peaks at a larger elongation. Thus, the detection rate is slightly higher from January to March and July to September when the apparent heliocentric distance of the peak in the lightcurve is largest. Only the very brightest comets are seen near the outer edges of C3, so the varying distance at which comets enter the field of view does not affect the discovery rate. The elongation as a function of heliocentric distance is plotted by month in Figure 18.

[FIGURE 18]

7.2.3. Phase Angle

Another effect of the geometry is the changing phase angle at which SOHO observes the comets at a given heliocentric distance. As discussed in Section 4.2, Kolokolova et al. (2004) and Marcus (2007b) found that the scattering of sunlight off of dust in the coma causes comets to brighten strongly due to forward-scattering at phase angles greater than 100° and to brighten slightly due to backscattering at phase angles smaller than 30°. The brightness at intermediate phase angles is relatively unchanged. A comet at phase angle ∼120° would appear brighter by ∼0.5 magnitude relative to a comet at 90° phase while a comet at ∼150° would appear brighter by ∼2.0 magnitudes relative to a comet at 90° phase (Marcus 2007b). Figure 19 shows the phase angle of Kreutz comets as a function of elongation on the 15^{th} of each month.

[FIGURE 19]

Comets which reach perihelion from September to January have phase angles greater than 100° for most or all of the time they are within the C3 field of view. Forward-scattering causes these comets to appear brighter than identical comets which reach perihelion from February to August, when they are at moderate phase (∼30°–100°) and experience minimal brightness enhancement due to phase. Thus, C3 detection rates are enhanced from September to January. Similarly, C2 detection rates are enhanced from August to December when comets are forward-scattering in the field of view. The brightening (and thus the increased detection rate) is strongly dependent on phase angle.

7.2.4. SOHO-centric Distance

A final effect of the geometry is that the comets are closer to the spacecraft from September to March than they are from April to August. At the extremes, comets which reach perihelion in November and December (when the SOHO-Sun line is nearly in the plane of the Kreutz orbit and comets approach from the near side of the Sun) are ∼10% closer than comets which reach perihelion in May and June (when the SOHO-Sun line is nearly in the plane of the Kreutz orbit and comets approach from the far side of the Sun). As a result, a comet which arrives in November or December would appear ∼0.2 magnitudes brighter than an identical comet which arrives in May or June. Thus, slightly more comets are detectable from September to March than from April to August. We summarize the seasonal effects in Table 5.

[TABLE 5]

7.3. True Arrival Rate

As discussed above, 2004–2007 is representative of the true detection rate of SOHO because during this period SOHO was continuously operational and the image cadence, duty cycle, and roll periods were nearly identical. Furthermore, amateur comet hunting was already well established on the Sungrazer website, and virtually all the comets were found in near real time (as opposed to pre-2000 discoveries which have been largely discovered in archival images, making it more difficult to be sure that all the images have been searched as thoroughly).

We use the four years 2004–2007, corrected for the duty cycle, as the true monthly discovery rates of SOHO. There is no reason to think the true flux varies from month to month, so we estimate the actual flux of Kreutz comets to be the average of the highest monthly detection rate (22.9 comets month^{-1}, in May). Therefore, we estimate the flux of Kreutz comets brighter than the threshold for observation by SOHO as $\sim$0.74 comets day^{-1}, or $\sim$270 comets year^{-1}. This is significantly higher than the rate of 14 comets month^{-1} found by Bzowski & Królikowska (2005) using data from 1997–2002 and the lower limit of 60 comets year^{-1} found by Biesecker et al. (2002), but is reflective of the improved discovery circumstances and the apparent overall increase in comet flux since then (discussed in the next section).

This rate is still only a lower limit as the spacecraft distance and phase angle effects discussed in Section 7.2 are sub-optimal during May. In principal, these effects could combine to improve the detection threshold by another 0.7 magnitudes (0.2 magnitudes due to the spacecraft distance and 0.5 magnitudes due to the phase angle). Since the size distribution of the Kreutz family heavily favors small comets, an ideal scenario where the viewing geometry and detector sensitivity are all aligned could yield $\sim$60% more comet detections, all at the

smal end of the size distribution.

7.4. Quantifying the Change in Comet Flux

While the number of Kreutz comets discovered by SOHO has increased since the beginning of the mission, we must correct for all of the changing detection biases before concluding that the flux has truly increased. First, we estimated the number of comets which were discovered due to a higher image cadence. From 1997–1998, an average of 42 C2 orange images and 25 C3 clear images were taken per day (the rates were lower in 1996 and most were not full resolution 1024×1024). We used this as a baseline and randomly removed images from the dataset of the comets discovered from 1999–2005 at a rate proportional to the average excess number of images in a given telescope per day for that year. For example, the rate of C2 orange images in 2001 was 63.3 images day^{-1}, or 21.3 images day^{-1} more than in 1997–1998. Thus, we removed 21.3/63.3=33.6% of the 2001 C2 orange images from our dataset. We created 10 such simulated datasets and compared the numbers of comets observed at different magnitudes, the length of observation, and the number of images in which the comet was observed. This allowed us to estimate the number of comets which would not have been discovered from 1997–1998 either because they did not reach the brightness threshold or because they were not observed in enough images due to the lower image cadence.

Next, we estimated the number of comets which have been discovered due to the roll of the telescope (starting in mid-2003) which would not have been discovered prior to then. Since 2004 the telescope has been rolled from roughly January to March, times when the occulting arm would obscure comets if the telescope was not rolled[27]. Since the raw number

[27]The date of the roll has moved approximately eight days earlier each year since 2004. This decreases the amount of time when the roll is favorable, and the raw total discoveries from January–March reflect this: 27

of comets discovered has increased as the mission has progressed, we took the ratio of the average number of detections from April to December in 2004–2008 relative to the average number of detections from April to December in 1999–2003 (the image cadence has been relatively stable since 1999 so we exclude the 1996–1998 data). We then multiplied this ratio by the average number of detections from January to March in 1999–2003, to estimate the number of comets we would have expected in January–March 2004–2008 based on the baseline increase in detections. Finally, we subtracted the expected number from the actual number detected to estimate the increase due to the telescope roll.

A final bias we attempted to correct for was the human element. In our calculation of the photometry of more than 900 comets, it subjectively appears that more comets of dubious quality have been discovered as the mission has progressed. This could be due to either changes in the SOHO team members confirming comet discoveries and reporting them to the IAU or an improvement in the ability of the amateurs discovering comets. Doug Biesecker was the primary SOHO team member who verified comet discoveries and reported them to the IAU through mid–2002, while Karl Battams has been the primary person in that position since then. The difference in personal bias in what constitutes a comet discovery could result in the increase in questionable comets. However, the number of SOHO "X-comets"[28], objects which show properties consistent with being a comet but lack sufficient evidence for a confirmation, have remained relatively constant at $\sim$5 comets year^{-1}. This suggests that the threshold for accepting an object as a comet has remained relatively constant throughout the mission, independent of the individual making the confirmations.

The amateurs discovering comets have unquestionably become more skilled at picking

---

in 2004, 26 in 2005, 22 in 2006, 20 in 2007, and 16 in 2008.

[28]http://sungrazer.nrl.navy.mil/index.php?p=xcomets.

faint comets out of the noise. It is unclear how thoroughly the archival data has been searched at these levels, and the increase in dubious detections may simply reflect that the data have been searched more thoroughly in recent years. Regardless of the cause, the number of comets whose brightest raw magnitude was fainter than 8 increased sharply during 2002–2003 and has remained high since. To quantify the increase, we averaged the number of comets year^{-1} fainter than magnitude 8 discovered from 1997–2001 (again ignoring 1996 due to its poor discovery circumstances). This was multiplied by the ratio of the number of comets brighter than magnitude 8 discovered from 2002–2005 relative to 1997–2001 to estimate the number of comets fainter than magnitude 8 that would be expected in 2002–2005 based on the overall increase in comet detections. Finally, we subtracted the expected number from the actual number of observed comets fainter than magnitude 8 from 2002–2005 to yield an estimate of the human bias.

Combining all of these effects, and dividing by the average combined C2 and C3 duty cycle for each year, we estimated the normalized number of detections for each year (Table 6). We included estimates for 2006–2008 (years for which we have not yet calculated photometry), where the increase due to the cadence was the average from 2004–2005, the increase due to the roll was calculated in the manner discussed above, and the increase due to human bias was the average from 2002–2005[29]. From 1997–2002 a corrected average of

[29]We have slightly altered the detection statistics for 1998 and 1999 from those given in Table 4. We have estimated the number of detections for July–October 1998 (SOHO was not operational from 1998 June 24 until 1998 October 22) as the average of the detection rates from July–October 1997 and 1999, and for January 1999 (SOHO was not operational from 1998 December 21 until 1999 February 2) as the average of the detection rate from January 1998 and 2000. Furthermore, the duty cycles listed for 1998 and 1999 are the duty cycles when the telescope was operational rather than the duty cycle for the whole year. Making these corrections decreases the estimates for 1998 and 1999 since the times when the spacecraft was inoperational are times when there are historically few comets discovered.

83.5±8.4 comets year^{-1} were discovered while from 2003–2008 124.2±7.3 comets year^{-1} were discovered. Even after correcting for the varying circumstances throughout the mission, the increase in discoveries remains evident.

[TABLE 6]

The jump in discoveries is not restricted to the faintest comets. The number of comets year^{-1} brighter than magnitude 6 increased from an average of 18.1±3.1 from 1997–2002 to 32.6±4.9 from 2003–2005, in increase of 80%. Comets magnitude 6 and brighter are typically observed for at least 24 hours and should have been easily discovered throughout the mission. Therefore the changing discovery circumstances should have little to no effect on the rate of discovery of these bright comets.

Sekanina & Chodas (2007) noted the increase in raw discoveries and suggested it may be "an early warning of another cluster of bright sungrazers approaching the Sun in coming decades." Our much more rigorous analysis of the detection statistics supports this finding. Coupled with the appearance in mid-2002 of comets with a rather intermediate lightcurve shape and peak distance (Section 5.1), their suggestion of "a nonuniform distribution of mini-comets along the filament" is plausible.

Could the increasing flux explain the existence of the largest fragments with the currently observed size distribution? In order to explain the largest comets seen from the ground, the number of comets year^{-1} would have to increase by a factor of ∼26. If the increase seen from 1997 to 2008 is sustained, it would require ∼80 years of sustained geometric increase or ∼750 years of sustained linear increase to reach the necessary flux of comets. Given that the Kreutz orbits are 500–1000 years, the presence of the largest fragments are only consistent with the geometric increase scenario (since the linear increase would need ∼1500 years before the average flux was large enough). If the largest comets are part of the SOHO observed

size distribution, then we must currently be at or very nearly at the absolute minimum in flux of Kreutz comets reaching perihelion.

7.5. Comparison with Previous Space-Based Coronagraphs

Nineteen Kreutz comets were discovered in SMM and Solwind images from 1979–1989, while Skylab observed for nine months in 1973–1974 without discovering any comets. The fields of view of Skylab (1.9–6 $R_\odot$), Solwind (2.5–10 $R_\odot$), and SMM (1.6 to between 4.8 and 6.5 $R_\odot$) were smaller than SOHO (Hundhausen et al. 1984; Howard et al. 1985), and the detectors were less sensitive. The estimated limiting magnitude was 6 for SMM (MacQueen & St. Cyr 1991), Skylab had "very similar capabilities [to SMM] for detection of coronal features" (Hundhausen et al. 1984), and the limiting magnitude of Solwind was likely $\sim$4 (discussed further below). Can these differences explain the much lower detection rate relative to SOHO, or is this further evidence of a nonuniform distribution of small comets around the orbit?

To compare the discovery rates of Skylab, Solwind, and SMM with the discovery rate of SOHO, we considered all comets which were seen by SOHO from 1996–2005 at elongations within the fields of view of Skylab, Solwind, and SMM. Because the SMM detectors were aligned in a diamond pattern with the Sun at the center and the cardinal directions at the vertices, the field of view varies substantially by position angle. We considered both the maximum and minimum elongations of SMM separately. We then determined the brightest point for the comet within each field of view, adding one magnitude to all orange magnitudes to correct for the orange–clear color difference (i.e. Section 5.3). The combined duty cycle for C2 and C3 from 1996-2005 was 0.868, or 8.68 years of effective observing time. We took the total number of comets seen by SOHO brighter than a particular magnitude in the

appropriate field of view (Skylab, Solwind, or SMM), divided by the effective observing time of SOHO, then multiplied by the effective observing time of the telescope (Skylab, Solwind, or SMM). This yielded the number of comets we would expect Skylab, Solwind, or SMM to have seen if the distribution of Kreutz comets reaching perihelion was the same as from 1996–2005. We additionally calculated the likelihood that a particular number of comets of a particular brightness would be seen by assuming the distribution was randomly distributed throughout the Kreutz orbit at the rate seen by SOHO and simulating the observing interval 10,000 times.

7.5.1. Skylab (1973–1974)

The Skylab coronagraph operated for 227 days, with an effective observing time of 93 days when a minimum of one observation per orbit was required for the duty cycle (Hundhausen et al. 1984). If we assume the limiting magnitude was 6 (as with SMM), then 1.1 comets would have been expected to be observed with a 33% chance of observing none if the comets were randomly distributed at the rate seen by SOHO. If instead the limiting magnitude was 4 we would have expected 0.4 comets to be observed with a 71% chance of observing none. Considering the short effective observation time and that the arrival times of Kreutz comets tend to be clustered (e.g. Marsden (1989); MacQueen & St. Cyr (1991)), the non-detection of comets in the Skylab dataset is not inconsistent with the SOHO observed size-distribution.

7.5.2. Solwind (1979–1985)

Solwind observed from March 1979 until September 1985. From publicly available images[30] we calculated the equivalent time that Solwind was observing during this time in a similar fashion as the duty cycle calculation for SOHO. We assumed that any gap in excess of 3 hours (the typical duration of Solwind comet observations) was lost time, then summed all the lost time and removed it from the total time that Solwind was observing. This yielded a total equivalent observing time of 4.4 years, somewhat higher than the equivalent observing time (3.6 years) that would be derived by using the duty cycle of 54.9% calculated by Howard et al. (1985) from 1979–1981 and applying it to the whole mission.

We use the magnitudes estimated on the discovery IAU circulars and those calculated by Rainer Kracht[31], yielding (in descending order of brightness): -4, -3, -2.5, -1.5[32], -0.8, 0.5, 2.5, 2.5, and 3.0 for the nine Kreutz comets observed by Solwind. Kracht, an expert comet hunter who has found more than 200 comets in coronagraphic images, methodically searched the Solwind images and found four comets which had not been discovered during the mission (Kracht & Marsden 2005a,b,c). Kracht reports that the faintest stars he could identify in Solwind images were magnitude 4.3–4.5 (private communication, 2008), thus we conservatively take the limiting magnitude to be 4.

Using the rate seen by SOHO, we would expect 14.7 comets magnitude 4 or brighter in the 4.4 years of equivalent observing for Solwind (nine were found), 2.6 comets magnitude 2 or brighter (six were found), and 0.5 comets magnitude 0 or brigher (five, and possibly six

---

[30]http://lasco-www.nrl.navy.mil/solwind/fits/.

[31]http://www.rkracht.de/solwind/index.htm.

[32]Solwind 5 = C/1984 O2 was also observed by SMM and was estimated to be magnitude -1.0 by MacQueen & St. Cyr (1991). For the purposes of these calculations either estimate will suffice.

considering the large uncertainties in brightness, were found). The total number of comets observed by Solwind is consistent with the SOHO distribution for comets magnitude 4 and brighter (23% chance of seeing nine or fewer comets magnitude 4 or brighter in 4.4 years if the distribution is uniform), however there were more bright comets than expected (2.0% chance of seeing six or comets magnitude 2 or brighter and 0.01% chance of seeing five or more comets magnitude 0 or brighter in 4.4 years).

7.5.3. SMM (1979, 1984–1989)

MacQueen & St. Cyr (1991) reviewed the 11 comets observed by SMM (ten discovered by SMM and one discovered by Solwind). All of these comets were observed at distances smaller than 10 $R_\odot$, most were observed for only ∼2 hours, and all were observed in six or fewer images. The lightcurves were flat or slightly increasing, the same phenomenon seen for the occasional comets observed at these distances in SOHO images (Biesecker et al. (2002), this work).

We calculated the equivalent time that SMM was observing from 1980–1989 in a similar fashion as the duty cycle calculation for SOHO using publicly available images[33]. We assumed that any gap in white light images (5000–5350 Å) in excess of 2 hours (the typical duration of SMM comet observations) was lost time, then summed all the lost time and removed it from the total time that SMM was observing[34]. This yielded a total equivalent observing

[33]http://smm.hao.ucar.edu/smm/smmcp_cme.html.

[34]Unlike Solwind and SOHO, SMM imaged the corona in four quadrants, with only one quadrant imaged at a time. Due to the geometry of the Kreutz orbit, comets were never seen in the "north" quadrant. Most were seen in the "west" and "south" quadrants, and a few in the "east" quadrant. Due to overlapping fields of view, some were seen in two quadrants. In calculating the duty cycle we ignored all "north" quadrant images, and required there to have been at least one "south", "east", and "west" image taken within 95 minutes

time of 4.6 years for SMM (MacQueen & St. Cyr (1991) used slightly different methodology and found 4.4 years).

We used the apparent magnitudes published by MacQueen & St. Cyr (1991) (in descending order of brightness: −2, −1, 0, +2, +2, +3, +3, +3, +5, +5, +6) as the peak magnitude for comparison with the SOHO rate. Using the smallest maximum elongation for the SMM detector and the equivalent observing time of 4.6 years, we would expect 12.2 comets magnitude 6 or brighter (11 were seen), 3.2 comets magnitude 3 or brighter (eight were seen), and 1.6 comets magnitude 1 or brighter (three were seen). Assuming the comets are distributed uniformly around the orbit, there is a 29% chance that 11 or fewer comets would be seen of magnitude 6 or brighter, a 0.2% chance that eight or more comets of magnitude 3 or brighter would be seen, and a 14% chance that three or more magnitude 1 or brighter comets would be seen. Using the largest maximum elongation for the SMM detector, we we expect 25.4 comets magnitude 6 or brighter, 4.8 comets magnitude 3 or brighter, and 2.1 comets magnitude 1 or brighter. Assuming the comets are distributed uniformly around the orbit, there is a 0.1% chance that 11 or fewer comets would be seen of magnitude 6 or brighter, a 1.4% chance that eight or more comets of magnitude 3 or brighter would be seen, and a 23% chance that three or more magnitude 1 or brighter comets would be seen.

(one orbit) of each other in order to consider each image for the duty cycle. A more rigorous determination of the duty cycle could account for the seasonal appearance of Kreutz comets in the quadrants. Removal of quadrants at the times when the Kreutz orbit cannot be seen in them would raise the equivalent observing time slightly but would not significantly affect the results.

7.5.4. Combined Dataset

To create a more robust dataset, we combined all the Kreutz comets discovered by space-based coronagraphs prior to SOHO. Taking a limiting magnitude for Solwind of 4 and using this as the threshold for detection by Skylab, Solwind, or SMM, 16 comets of the proper brightness were discovered. We combined the SMM and Solwind datasets and used two hours as the gap threshold throughout the missions. Combining these avoids double counting the period in 1984–1985 when both telescopes were observing (the only comet discovered during this time was observed by both telescopes). Adding the 93 equivalent days that Skylab observed yields an equivalent observing time of 8.0 years for the three coronagraphs. We would expect 17.3 comets during this time from the SOHO rate (using the smaller maximum SMM field of view) with 16 or more occuring 69% of the time if uniformly distributed. If instead we take the limiting magnitude of all three telescopes to be 1, eight comets were seen while we would expect 3.2 comets with only a 1.5% chance of detecting eight or more. Thus it appears that the total number of comets was about what would be expected based on the SOHO size-distribution, however the number of bright comets was too high. Changing the gap threshold, using the published duty cycles, or using the larger maximum SMM field of view produce only small changes to the equivalent observing time and expected number, and do not affect the conclusions.

7.5.5. Discussion

The statistical arguments above suggest that the distribution of SMM and Solwind comets differed from the distribution of SOHO comets. In both samples, there were an over-abundance of bright comets, although the total numbers of comets detected were reasonable. The baseline of observations for Skylab was too short to conclude that the distribution

was different from the SOHO distribution. Before drawing any conclusions regarding the distributions of these comets, we must first consider a number of assumptions made in these estimates.

Perhaps the most obvious concern is that the magnitudes of the comets and the limiting magnitudes of the telescopes have been estimated incorrectly. Stars of magnitude 6 can be seen in SMM images and are very similar in brightness to SMM-3 (1988p = C/1988 M1), whose brightness was estimated at magnitude 6. This comet was easy to see in a compressed JPG image, and it is doubtful that a significant number of comets this bright or brighter could have been missed (and certainly not more than 80% of them!). We feel it is unlikely that there is a substantial error in the magnitude to which the Solwind and SMM have been searched completely, as both have been search methodically by Rainer Kracht (private communication, 2008). For the Solwind and SMM comets to be consistent with the SOHO distribution, the brightness estimates of the brightest comets would need to be revised downward significantly while the fainter comets remained unchanged in brightness. Comparing the images of the first six Solwind discovered comets (the faintest of which was estimated to be magnitude 0.5) with the latter four discovered comets (the brightest of which was magnitude 1.5), the brighter comets are very obvious at a glance in the images while the the fainter comets are barely visible. Furthermore, the brightest six all have long, distinct tails while the four fainter comets have short, indistinct tails. In general, the presence and length of a tail in SOHO images are correlated with the brightness of the comet, and serve as additional confirmation that the brightest Solwind comets are distinctly brighter (and therefore larger) than the faintest Solwind comets. Considering the relative brightnesses of individual comets and the estimated uncertainty in brightness of ± 0.5 magnitudes (MacQueen & St. Cyr 1991) (and likely similar for Solwind), the magnitude estimates seem reasonable.

Even if the the limiting magnitudes of SMM and Solwind have been estimated correctly,

it is possible that there are comets above the threshold which have been missed in the images because they were only seen in one image. This is more likely for SMM with its smaller field of view; typical comets were seen in two or three images spanning ∼2 hours. Due to the apparently chaotic nature of the Kreutz lightcurve at small heliocentric distances (Biesecker et al. (2002), this work), a comet near the magnitude limit might be detectable in one image but not in the preceeding or subsequent images. This is more problematic for faint comets, as bright ones will likely stay above the threshold despite fluctuations in brightness. Furthermore, the brighter ones are more likely to have a visible tail, making them recognizable even if they are only observed in a single image. While comets were discovered in SMM and Solwind images with as as few as two images, at least three images would be necessary to confirm that a faint comet lacking a tail is not a cosmic ray. Depending on the image cadence and the amplitude of fluctuation in brightness of individual comets from image to image, the completeness of the SMM and Solwind detections likely varies near their respective limiting magnitudes.

Unfortunately there are a number of factors which limit the appropriateness of comparing the Solwind and SMM comet magnitudes with the SOHO comet magnitudes. First, the bandpasses of the Solwind (4100–6350 Å) and SMM (5000–5350 Å) filters are different from either the SOHO orange (5400–6400 Å) or clear filter (4000–8500 Å). The SMM bandpass does not include the known bright sodium doublet (5890 and 5896 Å) which is included in the other three. It is likely that the Solwind magnitudes would fall between the SOHO orange and clear magnitudes due to the widths of the bandpasses relative to the strong sodium emission while the SMM magnitude would be fainter than the SOHO clear magnitude due to the lack of the sodium emission line. This is consistent with the estimated magnitudes, as the Solwind comets were reported to be significantly brighter than the SMM comets, and the one comet seen by both (Solwind 5) was estimated to be 0.5 magnitude brighter

in Solwind. Our estimates of the number of comets which should have been seen in SMM and Solwind images were dependent on the magnitude limits being on the same scale as the SOHO clear filter. Thus, for direct comparison with the SOHO discovery rates, it is likely that the limiting magnitude of SMM was overestimated (the limiting magnitude should have been brighter) while the limiting magnitude of Solwind was underestimated (the limiting magnitude should have been fainter).

Second, no phase angle correction has been made. Phase corrections for both SMM and Solwind range from approximately −0.1 magnitudes (the comet would have appeared slightly brighter at 90° phase) to +2 magnitudes (the comet would have appeared much fainter at 90° phase)[35]. Applying phase corrections do not meaningfully alter the distribution of detections. They do make several of the brightest comets fainter, but not by enough to make the rate of bright comets observed by either telescope agree with the SOHO rate.

Next, no attempt has been made to correct the discovery rate for the vignetting of any of the telescopes. While this is likely to have a seasonal effect on the detection rate, it is unlikely to prevent the detection of the extremely bright comets, and should have little effect on the rate estimate. The magnitudes have not been normalized to unit spacecraft-centric distance, however there is typically less than a 3% difference from 1 AU, making a negligible difference in the magnitude estimates. Finally, there is the inherent uncertainty of the comet position, estimated at ± 0.1 $R_\odot$ for SMM (MacQueen & St. Cyr 1991), and likely similar for the Solwind comets. This uncertainty has a minimal effect on the magnitude estimate and can safely be ignored.

---

[35]It is difficult to estimate the phase correction for many of the SMM comets as the ephemeris generated by Horizons (http://ssd.jpl.nasa.gov/?horizons) differs substatially from some of the positions in Figure 6 of MacQueen & St. Cyr (1991), and the times of images given in some of the IAU circulars announcing the discoveries differ from those given on the image at the SMM C/P data archive.

Changing the assumptions made such as applying phase corrections or applying a magnitude correction to the SMM and Solwind magnitudes due to differing filter bandpasses do not substantially alter the conclusion that the SMM and Solwind comets have a different size distribution or frequency of arrival than the SOHO comets. However, given the myriad difficulties in comparing the Solwind and SMM comets with the SOHO comets and the likelihood that the datasets are not as complete at fainter magnitudes, we cannot say with certainty that the distributions are different.

7.5.6. Interpretation

There are several possible interpretations of the apparent higher rate of bright (i.e. large) comets reaching perihelion from 1979–1989 relative to 1996–2005. If we assume that the data were complete down to the estimated limiting magnitudes, then there were more large comets and fewer small comets (the size distribution was flatter) in the 1980s. In this case the size distribution was different from that seen by SOHO, and the distribution of "debris" (small comets) around the Kreutz orbit evidently changes on timescales as short as 10–15 years. This could be indicative of a different fragmentation process or possibly be evidence for constituents of the progenitor nucleus having accreted in different parts of the solar nebula, where the size distribution in each area was different.

Alternatively, if we assume that the SMM and Solwind data were incomplete at fainter magnitudes but had the same size distribution as the SOHO comets, then there were far more comets arriving in the 1980s than since 1996, with a tremendous population of comets fainter than magnitude 3–4 going undetected. Looking at the Solwind and SMM data separately, there were more bright comets arriving from 1979–1984 than from 1984–1989 (with the caveat that the sample size is extremely small). Combined with the apparent increase in

flux of SOHO comets beginning in 2003, this implies that the flux of comets varies around the orbit, and was likely in a local minimum during the 1990s. Since the most recent large, ground observed comets arrived between 1963–1970 this may mean that the Solwind and SMM comets were the end of the distribution of fragments scattered from these large comets while the increasing flux of SOHO comets presages a major fragment which will arrive in the next few decades. Since the majority of SOHO comets are subgroup I objects, this would suggest that the coming major fragment is of subgroup I.

A final interpretation is that the discoveries are relatively complete to the nominal limiting magnitudes, but because the lightcurves of individual comets are inherently chaotic at distances smaller than 6–8 $R_\odot$, the magnitudes of the comets seen by SMM and Solwind do not correspond to their sizes. This would be exacerbated by the short observing arcs and less frequent imaging of SMM and Solwind relative to SOHO's C2 coronagraph. In this scenario, we can only compare the overall rate of discovery and not the relative rate of bright versus faint comets. Then the Skylab, Solwind, and SMM discovery rates are consistent with those of SOHO and there has been minimal change in the flux of Kreutz comets reaching perihelion since at least 1979. Given the uncertainties inherent in comparing these differing datasets, we find this to be the most plausible explanation.

8. The Future of Kreutz Observations

8.1. STEREO

Although SOHO continues to operate, the next advance in space-based coronagraphs, Solar TErrestrial RElations Observatory (STEREO), is already in operation. STEREO is nominally a two year mission to observe the Sun in 3-D, with two identical spacecraft. One spacecraft orbits ahead (dubbed STEREO-A) and the other trails the Earth (dubbed

STEREO-B). They are gradually moving away from each other, and after two years will be 90° apart, each one 45° from the Earth (as viewed from the Sun). Each spacecraft has two coronagraphs (COR1 and COR2) and two heliospheric imagers (HI1 and HI2). COR1 has an annular field of view from 1.3–4.0 $R_\odot$ with a resolution of 7.5 arcsec pixel^{-1}, and a bandpass of 650–660 nm. COR2 has an annular field of view from 2–15 $R_\odot$ with a resolution of 15 arcsec pixel^{-1} and a bandpass of 650–750 nm. HI1 is centered 13.28° from the Sun with a circular 20° field of view, a resolution of 35 arcsec pixel^{-1}, and a bandpass of 650–750 nm. HI2 is centered 53.36° from the Sun with a circular 70° field of view, a resolution of 240 arcsec pixel^{-1}, and a bandpass of 400–1000 nm. The heliospheric imagers on STEREO-A look back at the Earth-Sun line, while the heliospheric imagers on STEREO-B look ahead at the Earth-Sun line (Kaiser 2005; Howard et al. 2008).

While the bandpasses, imaging sequences, and processing techniques are not as favorable for discovering comets as those of SOHO, STEREO recently discovered its first Kreutz comets which were apparently unobserved by SOHO (Battams et al. 2008). It has also observed a number of Kreutz comets which have also been seen by SOHO (e.g. Marsden & Battams (2008a,b); Marsden et al. (2008)). The additional observations yielded improved orbital calculations and increased lightcurve coverage. STEREO cannot rival SOHO in sheer quantity of sungrazer detections, but the quality of the observations of the comets it does observe is superior due to its smaller angular resolution over a larger range of distances relative to SOHO. Furthermore, it could help understand the lightcurve behavior at distances larger than 30 $R_\odot$ (beyond the SOHO field of view). Observations at these distances are likely to reveal a sharp increase in brightness from $\sim r^{-4}$ to $\sim r^{-7}$, and the heliocentric distance of this increase will give insight into the mechanism which causes it.

STEREO allows simultaneous imaging of comets from two different viewing geometries (three when combined with SOHO). This has already been used to derive the position of the

comet's tail in three dimensions using direct triangulation (Thompson 2009). This analysis revealed that the particles making up the tail were released 18–22 hours before perihelion (17–21 $R_\odot$) and confirmed that the tail shape can be characterized by a synchrone with no motion out of the plane (demonstrated using low resolution SOHO images by Sekanina (2000b)). Investigation of other well observed tails may demonstrate a link between the formation of a tail and the abrupt change in brightening slope seen between 20–30 $R_\odot$, and may improve estimates of the size of the dust particles.

Multiple viewing geometries will also allow a direct calculation of the scattering phase dependence by comparing the apparent magnitude of a comet as seen by each spacecraft. Understanding the dependence of the scattering on the phase angle will allow estimates of the sizes of typical particles in the coma and of the dust to gas ratio of the coma. This will also improve the correction of the apparent magnitudes in the SOHO field of view, since the comets Marcus (2007b) used to calculate the phase dependence were observed at much larger heliocentric distances and may have had different compositions, dust size distributions, and dust to gas ratios than do sungrazing comets.

8.2. Ground Based Telescopes

In the next few years, several large scale ground-based surveys are scheduled to begin collecting data: Pan-STARRS (Hawaii), LSST (Chile), and the Discovery Channel Telescope (Arizona). With the preponderance of large survey telescopes largely dedicated to searching for comets and near Earth objects, what are the chances that sungrazing comets will be observed from the ground?

A survey for Kreutz comets would look for them several months prior to perihelion. Due to the range of orbits, it is necessary to survey a wide area (at least 10 square degrees)

ideally with non-sidereal tracking at the expected rate of motion of the comets in that field of view. Because the comets are not known prior to being seen by SOHO, regions of the sky statistically likely to contain them must be chosen. The survey would ideally be carried out in the southern hemisphere with a telescope capable of imaging at relatively small solar elongations. Most of the planned surveys will observe too far from the Sun to discover Kreutz comets, although Pan-STARRS has plans to look for near-Earth objects at "sweet spots" some 60° from the Sun along the ecliptic which may be promising, although a comparable survey in the southern hemisphere would be preferable.

The magnitude of the Kreutz comets at these distances is unknown, but based on a preliminary search we undertook using the KPNO 4-m in January 2005, the rate of brightening is likely steeper than $\propto r^{-3.5}$. Even if the slope of the brightening is much steeper than this, the flux of Kreutz comets is large enough that we are hopeful that the occasional large comet will be detected. If such a comet were bright enough, high time resolution photometry might allow determination of the rotation rate and size. Discovery of a comet prior to its entering the SOHO field of view would allow the SOHO team to plan observing sequences such as cycling through the range of filters available on C2 and C3 (perhaps with a higher cadence and shorter observing times since the brightest comets saturate the detector) and alignment of the UVCS spectrograph, all of which could give insight into the composition.

9. Summary

This work has investigated the lightcurves of more than 900 Kreutz comets seen by SOHO from 1996–2005. While the information available from a single comet lightcurve is often minimal, studying them collectively has allowed us to draw conclusions about the Kreutz group as a whole. The Kreutz comets observed by SOHO have a power-law size distribution

and they have a continuum of slightly different compositions. The individual lightcurves follow a similar shape, but differ individually due to each comet's unique composition, fragmentation history, shape, and rotation period. It appears that the distribution of these small comets is not uniform around the orbit. We summarize the key results below.

- The lightcurves do not have a bimodal distance of peak brightness as previously reported by Biesecker et al. (2002). Instead, they reach a peak in brightness over a range from 10.5–14 $R_\odot$ with a maximum around 12 $R_\odot$. This suggests that there is a continuum of compositions among the members rather than two distinct compositions.

- Most lightcurves brighten near $\propto r^{-7.3}$ when they first become visible then exhibit a change in brightening rate between 20–30 $R_\odot$, brightening near $\propto r^{-3.8}$ from 16–24 $R_\odot$. It is unclear how far outward the $\propto r^{-7.3}$ extends. The rate of brightening from 16–24 $R_\odot$ is similar to the rates of fading of the ground observed members of the family as well as the canonical rate of brightening for most comets. The increased activity which results in the steeper lightcurve when first visible may be responsible for tail formation.

- The comets appear brighter in the C2 and C3 orange filters than the C3 clear filter by $\sim$1 magnitude, although the difference varies with heliocentric distance, reaching a maximum near 19 $R_\odot$. We concur with previous authors (e.g. Biesecker et al. (2002); Sekanina (2003)) that this difference in brightness is due to sodium emission, however the mass of sodium required to cause this brightness increase is high compared to the lower limit for the size of these comets.

- The size range is 2–50 meters in radius, although due to a number of simplifying assumptions the comet may be a factor of two larger or smaller. The cumulative size distribution is $N(>R) \propto R^{-2.2}$. The largest fragment in this distribution should be $\sim$500 meters in radius, consistent with C/1887 B1 and C/1945 X1 (the two smallest

ground observed Kreutz comets) being the two largest members of the group. Six other ground observed comets were much larger than this. If the distribution of comets seen by SOHO is consistent throughout the orbit, there are ∼20,000 comets larger than 5 meters. These would have a total mass of $\sim 4 \times 10^{14}$ g which is much smaller than the likely mass of the largest ground observed members. From these arguments we conclude that either the size distribution does not extend to the largest sizes, or that the distribution is not uniform around the orbit.

- The flux of Kreutz comets reaching perihelion has increased during the mission. After correcting for the changing discovery circumstances, the average comets year^{-1} increased from 83.5±8.4 from 1997–2002 to 124.2±7.3 from 2003–2008. The increase is not restricted to the smallest comets, as there was an 80% increase in comets brighter than magnitude 6, suggesting the increase is due to a changing distribution around the orbit rather than an improvement in the discovery capabilities.

- There were more bright (large) comets observed with Solwind and SMM from 1979–1989 than would be expected from the SOHO data. Depending on the completeness of these datasets at fainter magnitudes, this may be due to a flatter size distribution or a different flux of comets reaching perihelion. However, due to the large uncertainties in comparing the datasets (most notably the apparent magnitudes) we cannot rule out the possibility that the Kreutz distribution has remained relatively constant since 1979.

- While SOHO is operational it will continue to dominate the discovery of Kreutz comets, however STEREO provides higher quality data over a larger range of distances for the comets it does observe. STEREO observations should help to understand the typical lightcurve at distances larger than 30 $R_\odot$ and should allow a more robust determination of scattering at large phase angles. Ground-based surveys may discover a small number

of Kreutz comets. If recognized in a timely fashion, such discoveries would allow subsequent follow-up observation from the ground and special observing sequences by SOHO which may help constrain the size, rotation state, and composition.

Acknowledgements

We would like to thank the members of the SOHO and STEREO teams who have helped at many stages of this work, especially Derek Hammer and Karl Battams who have maintained the official sungrazer website since Doug Biesecker left. We would also like to thank the many comet hunters who have made it possible to study nearly an order of magnitude more comets in this work than any paper to date. In particular we would like to thank Rainer Kracht for his helpful insight over the years. This work was supported by NASA Planetary Atmospheres grants NAG513295 and NNG06GF29G.

REFERENCES

A'Hearn, M. F., Belton, M. J. S., Delamere, W. A., Kissel, J., Klaasen, K. P., McFadden, L. A., Meech, K. J., Melosh, H. J., Schultz, P. H., Sunshine, J. M., Thomas, P. C., Veverka, J., Yeomans, D. K., Baca, M. W., Busko, I., Crockett, C. J., Collins, S. M., Desnoyer, M., Eberhardy, C. A., Ernst, C. M., Farnham, T. L., Feaga, L., Groussin, O., Hampton, D., Ipatov, S. I., Li, J.-Y., Lindler, D., Lisse, C. M., Mastrodemos, N., Owen, W. M., Richardson, J. E., Wellnitz, D. D., & White, R. L. 2005, Science, 310, 258

Battams, K., Baldwin, K., & Marsden, B. G. 2008, IAU Circ., 8926

Bemporad, A., Poletto, G., Raymond, J. C., Biesecker, D. A., Marsden, B., Lamy, P., Ko, Y.-K., & Uzzo, M. 2005, ApJ, 620, 523

Biesecker, D. A., Lamy, P., St. Cyr, O. C., Llebaria, A., & Howard, R. A. 2002, Icarus, 157, 323

Brueckner, G. E., Howard, R. A., Koomen, M. J., Korendyke, C. M., Michels, D. J., Moses, J. D., Socker, D. G., Dere, K. P., Lamy, P. L., Llebaria, A., Bout, M. V., Schwenn, R., Simnett, G. M., Bedford, D. K., & Eyles, C. J. 1995, Sol. Phys., 162, 357

Bzowski, M., & Królikowska, M. 2005, A&A, 435, 723. arXiv:astro-ph/0405148

Curtis, G. W., & The Sacramento Peak Observatory Staff 1966, AJ, 71, 194

England, K. J. 2002, Journal of the British Astronomical Association, 112, 13

Evans, C., & McKim Malville, J. 1967, PASP, 79, 310

Fernández, J. A., Tancredi, G., Rickman, H., & Licandro, J. 1999, A&A, 352, 327

Fernández, Y. R., Lisse, C. M., Kelley, M. S., Dello Russo, N., Tokunaga, A. T., Woodward, C. E., & Wooden, D. H. 2007, Icarus, 191, 424

Gehrz, R. D., & Ney, E. P. 1992, Icarus, 100, 162

Groussin, O., A'Hearn, M. F., Li, J.-Y., Thomas, P. C., Sunshine, J. M., Lisse, C. M., Meech, K. J., Farnham, T. L., Feaga, L. M., & Delamere, W. A. 2007, Icarus, 187, 16

Grynko, Y., Jockers, K., & Schwenn, R. 2004, A&A, 427, 755

Hasegawa, I. 1966, The Heavens (in Japanese), 47, 31

Hasegawa, I., & Nakano, S. 2001, PASJ, 53, 931

Howard, R. A., Moses, J. D., Vourlidas, A., Newmark, J. S., Socker, D. G., Plunkett, S. P., Korendyke, C. M., Cook, J. W., Hurley, A., Davila, J. M., Thompson, W. T., St Cyr, O. C., Mentzell, E., Mehalick, K., Lemen, J. R., Wuelser, J. P., Duncan, D. W., Tarbell, T. D., Wolfson, C. J., Moore, A., Harrison, R. A., Waltham, N. R., Lang, J., Davis, C. J., Eyles, C. J., Mapson-Menard, H., Simnett, G. M., Halain, J. P., Defise, J. M., Mazy, E., Rochus, P., Mercier, R., Ravet, M. F., Delmotte, F., Auchere, F., Delaboudiniere, J. P., Bothmer, V., Deutsch, W., Wang, D., Rich, N., Cooper, S., Stephens, V., Maahs, G., Baugh, R., McMullin, D., & Carter, T. 2008, Space Science Reviews, 136, 67

Howard, R. A., Sheeley, N. R., Jr., Michels, D. J., & Koomen, M. J. 1985, J. Geophys. Res., 90, 8173

Hundhausen, A. J., Sawyer, C. B., House, L., Illing, R. M. E., & Wagner, W. J. 1984, J. Geophys. Res., 89, 2639

Iseli, M., Küppers, M., Benz, W., & Bochsler, P. 2002, Icarus, 155, 350. arXiv:astro-ph/0110091

Jewitt, D. 1991, in IAU Colloq. 116: Comets in the Post-Halley Era, edited by R. L. Newburn, Jr., M. Neugebauer, & J. Rahe, vol. 167 of Astrophysics and Space Science Library, 19

Kaiser, M. L. 2005, Advances in Space Research, 36, 1483

Kimura, H., Mann, I., Biesecker, D. A., & Jessberger, E. K. 2002, Icarus, 159, 529

Kirkwood, D. 1880, The Observatory, 3, 590

Knight, M. M., Walsh, K. J., A'Hearn, M. F., Swaters, R. A., Zauderer, B. A., Samarasinha, N. H., Vázquez, R., & Reitsema, H. 2007, Icarus, 187, 199

Kolokolova, L., Hanner, M. S., Levasseur-Regourd, A.-C., & Gustafson, B. Å. S. 2004, in Comets II, edited by M. C. Festou, H. U. Keller, & H. A. Weaver (Univ. of Arizona Press/Lunar Planet. Inst., Tucson, AZ/Houston, TX), 577

Kracht, R., & Marsden, B. G. 2005a, IAU Circ., 8566

— 2005b, IAU Circ., 8583

— 2005c, IAU Circ., 8573

Kresák, L. 1966, Bulletin of the Astronomical Institutes of Czechoslovakia, 17, 188

Kreutz, H. 1888, Untersuchungen Über das Cometensystem 1843 I, 1880 I und 1882 II. (Kiel, Druck von C. Schaidt, C. F. Mohr nachfl., 1888.)

— 1891, Publication der Koeniglichen Sternwarte in Kiel, 6

— 1901, Astronomische Nachrichten, 155, 63

Lamy, P., Biesecker, D. A., & Groussin, O. 2003, Icarus, 163, 142

Lamy, P. L., Toth, I., Fernandez, Y. R., & Weaver, H. A. 2004, in Comets II, edited by M. C. Festou, H. U. Keller, & H. A. Weaver (Univ. of Arizona Press/Lunar Planet. Inst., Tucson, AZ/Houston, TX), 223

Lisse, C. M., VanCleve, J., Adams, A. C., A'Hearn, M. F., Fernández, Y. R., Farnham, T. L., Armus, L., Grillmair, C. J., Ingalls, J., Belton, M. J. S., Groussin, O., McFadden, L. A., Meech, K. J., Schultz, P. H., Clark, B. C., Feaga, L. M., & Sunshine, J. M. 2006, Science, 313, 635

Llebaria, A., Lamy, P., & Danjard, J.-F. 2006, Icarus, 182, 281

Lowry, S., Fitzsimmons, A., Lamy, P., & Weissman, P. 2008, Kuiper Belt Objects in the Planetary Region: The Jupiter-Family Comets, 397

MacQueen, R. M., & St. Cyr, O. C. 1991, Icarus, 90, 96

Marcus, J. N. 2007a, IAU Circ., 8793

— 2007b, Int. Comet Quart., 39

— 2007c, Int. Comet Quart., 119

Marcus, J. N., & Seargent, D. A. J. 1986, in ESLAB Symposium on the Exploration of Halley's Comet. Volume 2: Dust and Nucleus, vol. 250 of ESA Special Publication, 359

Marsden, B. G. 1967, AJ, 72, 1170

— 1989, AJ, 98, 2306

Marsden, B. G., & Battams, K. 2008a, Minor Planet Electronic Circulars, F38

— 2008b, Minor Planet Electronic Circulars, G4

Marsden, B. G., Battams, K., & Baldwin, K. 2008, Minor Planet Electronic Circulars, G15

Meech, K. J., Hainaut, O. R., & Marsden, B. G. 2004, Icarus, 170, 463

Michels, D. J., Sheeley, N. R., Howard, R. A., & Koomen, M. J. 1982, Science, 215, 1097

Morrill, J. S., Korendyke, C. M., Brueckner, G. E., Giovane, F., Howard, R. A., Koomen, M., Moses, D., Plunkett, S. P., Vourlidas, A., Esfandiari, E., Rich, N., Wang, D., Thernisien, A. F., Lamy, P., Llebaria, A., Biesecker, D., Michels, D., Gong, Q., & Andrews, M. 2006, Sol. Phys., 233, 331

Ney, E. P. 1982, in IAU Colloq. 61: Comet Discoveries, Statistics, and Observational Selection, edited by L. L. Wilkening, 323

Ney, E. P., & Merrill, K. M. 1976, Science, 194, 1051

Preston, G. W. 1967, ApJ, 147, 718

Raymond, J. C., Fineschi, S., Smith, P. L., Gardner, L., O'Neal, R., Ciaravella, A., Kohl, J. L., Marsden, B., Williams, G. V., Benna, C., Giordano, S., Noci, G., & Jewitt, D. 1998, ApJ, 508, 410

Schulz, R., Owens, A., Rodriguez-Pascual, P. M., Lumb, D., Erd, C., & Stüwe, J. A. 2006, A&A, 448, L53

Sekanina, Z. 1967a, Bulletin of the Astronomical Institutes of Czechoslovakia, 18, 229

— 1967b, Bulletin of the Astronomical Institutes of Czechoslovakia, 18, 198

— 2000a, ApJ, 542, L147

— 2000b, ApJ, 545, L69

— 2002a, ApJ, 576, 1085

— 2002b, ApJ, 566, 577

— 2003, ApJ, 597, 1237

Sekanina, Z., & Chodas, P. W. 2002a, ApJ, 581, 760

— 2002b, ApJ, 581, 1389

— 2004, ApJ, 607, 620

— 2007, ApJ, 663, 657

— 2008, ApJ, 687, 1415

Sheeley, N. R., Jr., Howard, R. A., Koomen, M. J., & Michels, D. J. 1982, Nature, 300, 239

Slaughter, C. D. 1969, AJ, 74, 929

Snodgrass, C., Fitzsimmons, A., Hainaut, O., Hamuy, M., Hutsemekers, D., Jehin, E., Jones, M., & Manfroid, J. 2007, Central Bureau Electronic Telegrams, 832

Spinrad, H., & Miner, E. D. 1968, ApJ, 153, 355

Strom, R. 2002, A&A, 387, L17

Sunshine, J. M., Groussin, O., Schultz, P. H., A'Hearn, M. F., Feaga, L. M., Farnham, T. L., & Klaasen, K. P. 2007, Icarus, 190, 284

Tancredi, G., Fernández, J. A., Rickman, H., & Licandro, J. 2006, Icarus, 182, 527

Thernisien, A. 2003, private communication

Thernisien, A. F., Morrill, J. S., Howard, R. A., & Wang, D. 2006, Sol. Phys., 233, 155

Thompson, W. T. 2009, Icarus, 200, 351

Uzzo, M., Raymond, J. C., Biesecker, D., Marsden, B., Wood, C., Ko, Y.-K., & Wu, R. 2001, ApJ, 558, 403

Watanabe, J.-i., Kawakita, H., Furusho, R., & Fujii, M. 2003, ApJ, 585, L159

Weidenschilling, S. J. 2004, in Comets II, edited by M. C. Festou, H. U. Keller, & H. A. Weaver (Univ. of Arizona Press/Lunar Planet. Inst., Tucson, AZ/Houston, TX), 97

Weissman, P. R. 1983, Icarus, 55, 448

Weissman, P. R., & Lowry, S. C. 2003, in Lunar and Planetary Institute Conference Abstracts, edited by S. Mackwell, & E. Stansbery, vol. 34, 2003

Telescope	Field of View ($R_\odot$)	Occulter Type	Spectral Bandpass	Pixel Size (arcsec)	Brightness Range($B_\odot$)
C1	1.1–3.0	Internal	Fabry-Perot	5.6	2×10^{-5} – 2×10^{-8}
C2	2.0–6.0	External	Broadband	11.9	2×10^{-7} – 5×10^{-10}
C3	3.7–30	External	Broadband	56.0	3×10^{-9} – 5×10^{-11}

Table 1: Specifications for the C1, C2, and C3 telescopes. Reproduced from Table I in Brueckner et al. (1995).

Table 2:: Comets which have a reliably determined peak in C3. The distance of the peak is likely only good to ±0.5 $R_\odot$. The apparent visual magnitude of the peak is given for C3 and for C2 when possible. When the C2 peak is not visible, the maximum observed brightness in C2 is listed. The group identification is based on the shape of the lightcurve as discussed in Section 5.1. Comets are listed in order of perihelion time. The comets which are italicized saturated the detector. The internal SOHO numbers are included for comparison with Biesecker et al. (2002).

Designation	SOHO #	Distance of Peak ($R_\odot$)	C2 Peak Magnitude	C3 Peak Magnitude	Group
C/1996 O4	23	12.3	—	5.4	C
C/1996 Q3	2	11.5	—	6.4	C
C/1996 S3	3	13.0	—	5.5	A
C/1997 L3	12	10.6	—	5.0	C
C/1997 M1	15	11.1	—	5.7	C
C/1997 P1	19	12.6	—	3.3	A
C/1997 Q2	25	12.8	—	4.3	A
C/1997 T2	31	10.9	<5.6	6.4	C
C/1998 G4	47	11.4	<3.8	4.6	C
C/1998 H2	48	13.0	<1.1	2.1	A
C/1998 K10	*54*	*10.8*	*0.6*	*0.8*	—
C/1998 K11	*55*	*10.9*	*0.1*	*0.5*	—
C/1998 L1	56	12.8	<5.5	5.4	B
C/1999 C1	58	12.5	—	5.4	A
C/1999 O3	74	11.7	—	5.7	C
C/1999 S1	86	12.6	—	4.8	A
C/2000 B1	97	12.3	—	4.3	A
C/2000 B6	98	11.3	—	6.3	C
C/2000 C6	104	11.1	—	5.2	C
C/2000 D1	106	11.2	—	5.1	C
C/2000 E1	107	12.2	—	5.3	A
C/2000 H2	*111*	*9.7*	*0.5*	*0.7*	—
C/2000 T1	204	12.9	<3.4	4.3	A
C/2001 C3	293	11.6	—	5.9	A
C/2001 C2	294	12.1	—	4.2	A
C/2001 C6	296	10.8	<5.6	5.3	C
C/2001 R2	*347*	*12.8*	*<3.8*	*2.9*	—
C/2001 U4	361	13.7	<6.3	7.3	A
C/2001 U7	365	14.0	<4.3	5.5	A

Continued on next page

Table 2 – continued from previous page

Designation	SOHO #	Distance of Peak ($R_\odot$)	C2 Peak Magnitude	C3 Peak Magnitude	Group
C/2001 U9	*367*	*13.1*	*<1.4*	*2.8*	—
C/2002 J3	443	10.7	<2.9	4.1	C
C/2002 Q7	503	12.3	—	5.6	B
C/2002 S2	517	12.4	<4.0	3.7	B
C/2002 W12	556	12.5	<4.8	6.4	A
C/2003 A3	579	11.8	—	5.4	A
C/2003 C2	584	12.3	—	4.0	A
C/2003 C5	587	12.1	—	6.4	B
C/2003 F3	592	12.8	<4.2	4.4	C
C/2003 F5	594	12.6	<3.0	3.8	A
C/2003 K7	*614*	*10.8*	*-0.0*	*-0.1*	—
C/2003 L5	624	12.9	3.0	4.0	B
C/2003 O5	644	11.1	<5.0	4.2	C
C/2003 Q2	652	12.3	—	5.2	A
C/2003 Q5	655	11.9	—	4.9	C
C/2003 Q7	657	11.5	—	4.5	C
C/2003 V5	687	12.0	<4.8	5.9	A
C/2003 W6	694	12.0	<4.4	6.0	A
C/2004 A2	724	12.0	—	4.7	B
C/2004 D4	744	12.9	—	4.5	A
C/2004 F6	750	12.3	<5.0	5.3	A
C/2004 O1	819	11.8	—	4.8	B
C/2004 P7	828	12.2	—	5.8	B
C/2004 Q3	829	12.0	—	6.3	B
C/2004 Q4	830	11.8	—	6.1	B
C/2004 R4	833	12.7	—	5.8	B
C/2004 T7	844	11.5	<5.5	6.9	B
C/2005 C3	907	11.3	—	5.0	B
C/2005 D5	913	12.2	<6.4	5.5	A
C/2005 E6	917	11.3	<5.9	5.3	C
C/2005 F1	925	10.8	<6.2	6.2	B
C/2005 L7	972	11.1	3.3	4.3	B
C/2005 N9	993	12.6	<5.5	5.2	B
C/2005 O3	995	12.3	<6.2	4.5	A
C/2005 P1	999	12.2	—	6.5	A
C/2005 S1	1024	13.7	<3.8	4.1	A
C/2005 T11	1031	13.2	<5.3	5.8	A
C/2005 V9	1047	12.2	<4.0	4.9	A
C/2005 Y9	1078	12.2	<4.9	6.3	A
C/2006 A5	1087	11.7	<3.7	3.9	A
C/2006 B3	1091	11.2	—	6.2	A
C/2006 B6	1094	11.2	—	5.8	C

Parameter	Raw data (median ± SIQR)	Corrected data (median ± SIQR)
Peak Distance ($R_\odot$)	11.9 ± 0.45	12.2 ± 0.55
Slope of C2 orange fading from 10–7 $R_\odot$	−5.1 ± 0.9	−5.5 ± 1.2
Slope of C3 clear fading from 10–7 $R_\odot$	−3.9 ± 0.9	−3.9 ± 0.7
Slope of C3 clear brightening from 24–16 $R_\odot$	+3.9 ± 0.6	+3.8 ± 0.7
Slope of C3 clear brightening beyond 24 $R_\odot$	+8.0 ± 1.9	+7.3 ± 2.0
Slope of size distribution	−2.22	−2.22
Median orange – clear magnitude difference	−1.03 ± 0.30	−1.19 ± 0.34

Table 3: The effects on the lightcurve properties of normalizing the photometry to a unit SOHO-centric distance and correcting for phase angle.

Year	C2	C3	Total
1996	9	26	27
1997	55	31	69
1998	66	17	70
1999	53	33	71
2000	69	32	79
2001	77	32	84
2002	91	38	106
2003	98	65	132
2004	105	84	146
2005	117	86	143
2006	114	72	141
2007	125	80	150
2008	113	67	135
Total	1092	663	1353

Table 4: Yearly SOHO Kreutz discoveries by telescope from 1996–2007. Note that many comets are seen in both C2 and C3. Therefore the combined total is less than the sum of the individual telescopes.

Effect	When	C2 Discovery Rate	C3 Discovery Rate
Occulting arm	Jan–May	small decrease	large decrease
Telescope roll	every 3 months	small increase when rolled in Jan–May	large increase when rolled in Jan–May
SOHO-Sun line nearly in plane of Kreutz orbit	Apr–Jun & Oct–Dec	large increase	slight decrease
SOHO-Sun line nearly perpendicular to plane of Kreutz orbit	Jan–Mar & Jul–Sep	large decrease	slight increase
Phase angle	Sep–Jan	no change	increase
Phase angle	Aug–Dec	increase	no change
SOHO-comet dist <1 AU	Sep–Mar	slight increase	slight increase
SOHO-comet dist >1 AU	Apr–Aug	slight decrease	slight decrease

Table 5: Summary of seasonal effects on detection rate.

Year	Actual Number	Extra Due to Increased Cadence	Extra Due to Roll	Extra Due to Human Bias	Net Number	Duty Cycle	Corrected Number
1996	27	0	0	0	27.0	0.735	36.7
1997	69	0	0	0	69.0	0.946	72.9
1998	92[a]	0	0	0	92.0	0.928[b]	99.1
1999	74[a]	1.6	0	0	72.4	0.862[b]	84.0
2000	79	8.9	0	0	70.1	0.944	74.3
2001	84	9.7	0	0	74.3	0.944	78.7
2002	106	16.5	0	6.2	83.3	0.957	87.0
2003	131	12.7	0	4.2	114.1	0.917	124.4
2004	146	11.3	12.7	8.2	113.7	0.888	128.1
2005	143	19.0	10.7	5.2	108.0	0.964	112.1
2006	141	15.2	7.7	6.0	112.1	0.893	125.6
2007	150	15.2	5.7	6.0	123.1	0.920	133.9
2008	135	15.2	0.7	6.0	113.1	0.932	121.4

[a] The number of comets discovered in 1998 and 1999 has been extrapolated to fill in the data gaps due to spacecraft failure. See the footnote in the text for more information.

[b] The duty cycles for 1998 and 1999 are the average duty cycles during the times when the telescope was operational (i.e. excluding the gaps due to spacecraft failure). See the footnote in the text for more information.

Table 6: Detection rates corrected for the varying detection biases. Column 1 is the year. Column 2 is the actual number of comets discovered. Column 3 is the estimated number of comets that were discovered due to the higher image cadence than in 1996–1998. Column 4 is the estimated number of comets that were discovered due to the roll of the telescope. Column 5 is the estimated number of comets that were accepted as comets due to changing human bias. Column 6 is the net number of discoveries after subtracting the increases (columns 3–5). Column 7 is the duty cycle, and Column 8 is the number of detections after correcting the net number for the duty cycle.

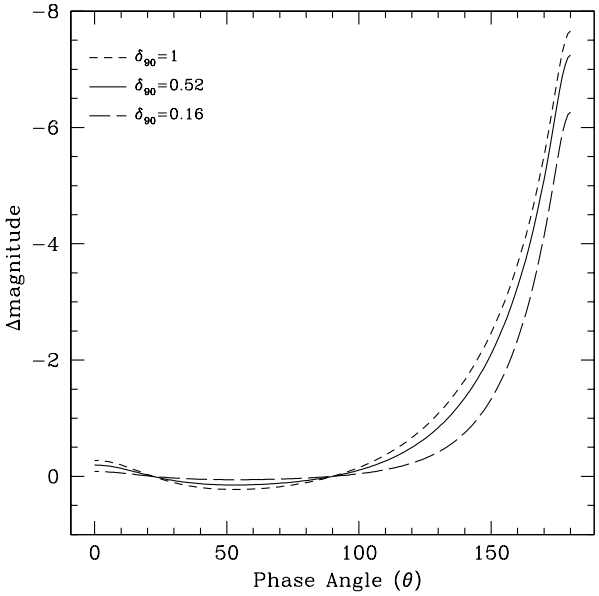

Fig. 1.— Marcus (2007b) phase function as given by Equation 5. Three dust-to-gas light ratios (δ_{90}) are plotted: 1 (dashed line), 0.52 (solid line), and 0.16 (long-dashed line).

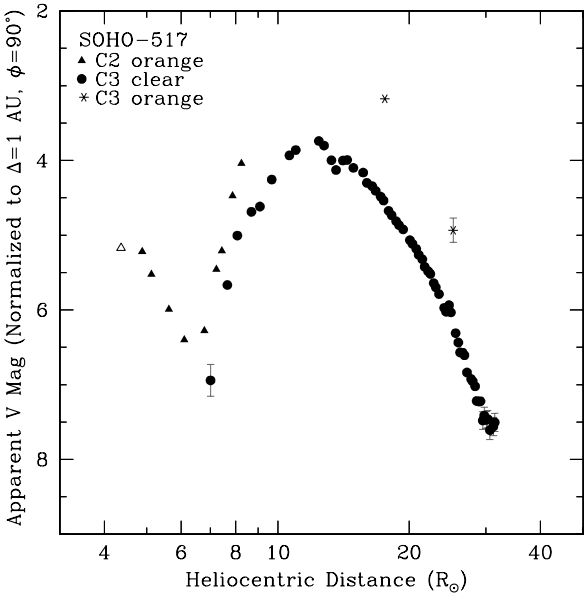

Fig. 2.— Lightcurve of C/2002 S2 (SOHO-517) which is representative of the typical Kreutz lightcurve shape. The triangles are C2 orange filter images, circles are C3 clear filter images, and asterisks are C3 orange filter images. The open points are images which had vignetting greater than 4.0. Error bars smaller than 0.1 magnitudes (for the upper error bar) have been suppressed.

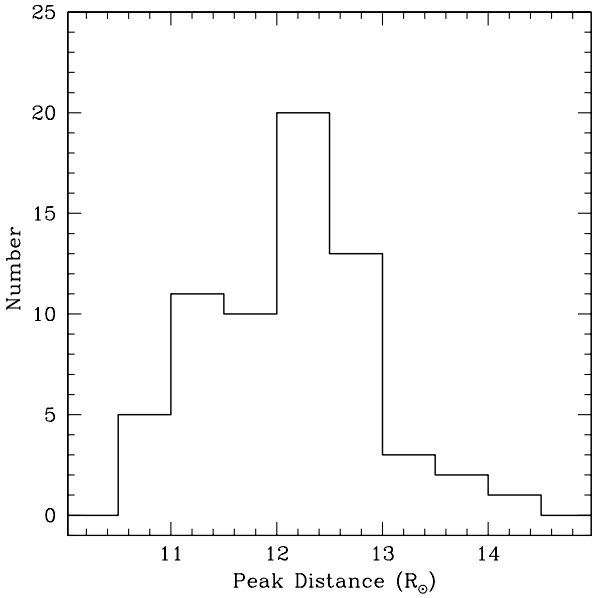

Fig. 3.— Histogram of the heliocentric distance of peak brightness for comets observed to peak in C3.

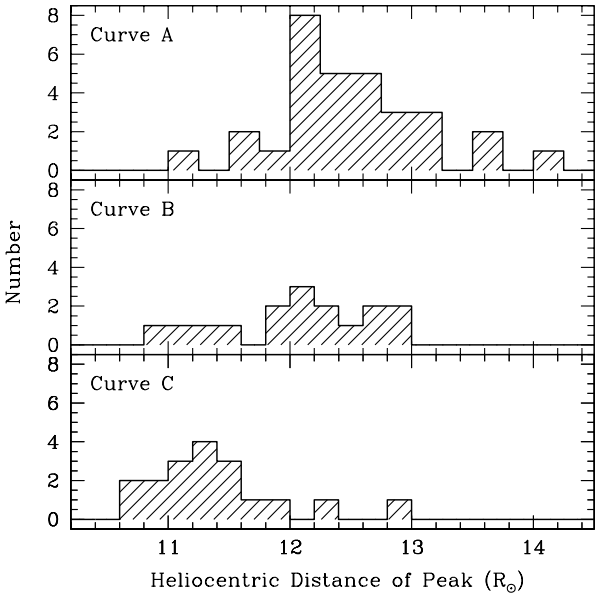

Fig. 4.— Histogram of the heliocentric distance of peak brightness for the three characteristic shapes of brightening. The top panel is curve A, the middle panel is curve B, and the bottom panel is curve C.

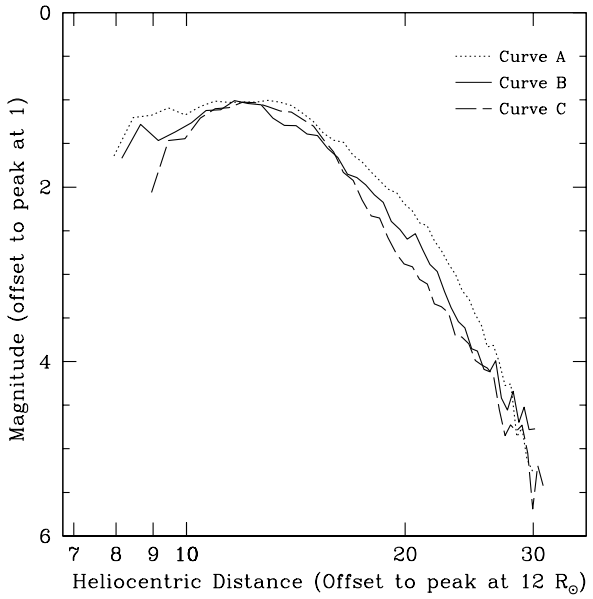

Fig. 5.— Plots of the three characteristic curves normalized so that they all peak at a magnitude of 1 and a heliocentric distance of 12 $R_{\odot}$. Curve A is the dotted line, curve B is the solid line, and curve C is the dashed line.

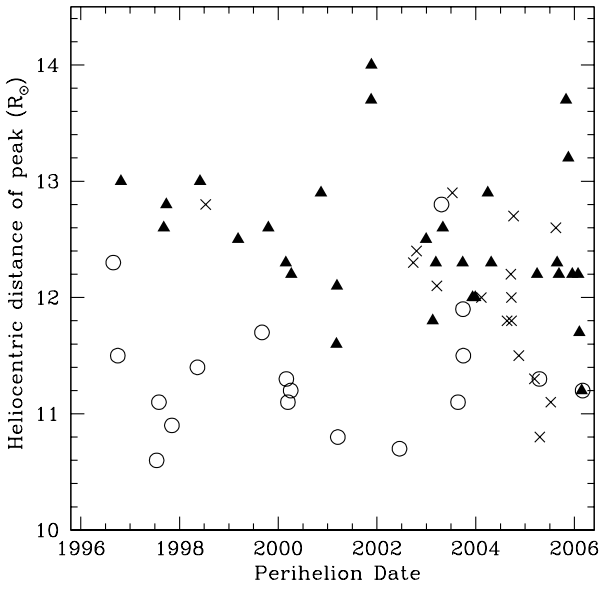

Fig. 6.— Perihelion date versus heliocentric distance of the peak magnitude for the comets observed to peak in C3. The triangles are in curve A, crosses are in curve B, and circles are in curve C.

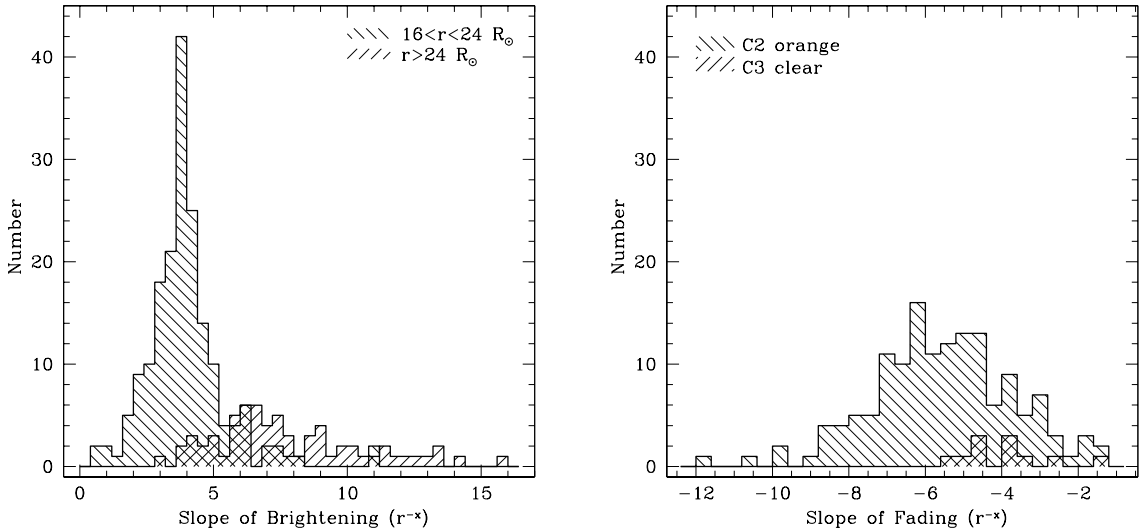

Fig. 7.— Histograms of the slope of the brightening (left panel) and fading (right panel) of Kreutz comets. The slopes of brightening are calculated for two regions in the C3 clear filter: distances larger than 24 $R_\odot$ (hatching at +45°) and from 24–16 $R_\odot$ (hatching at −45°). The slopes of fading are calculated from 10–7 $R_\odot$ for the C3 clear filter (hatching at +45°) and the C2 orange filter (hatching at −45°). All distances are prior to perihelion.

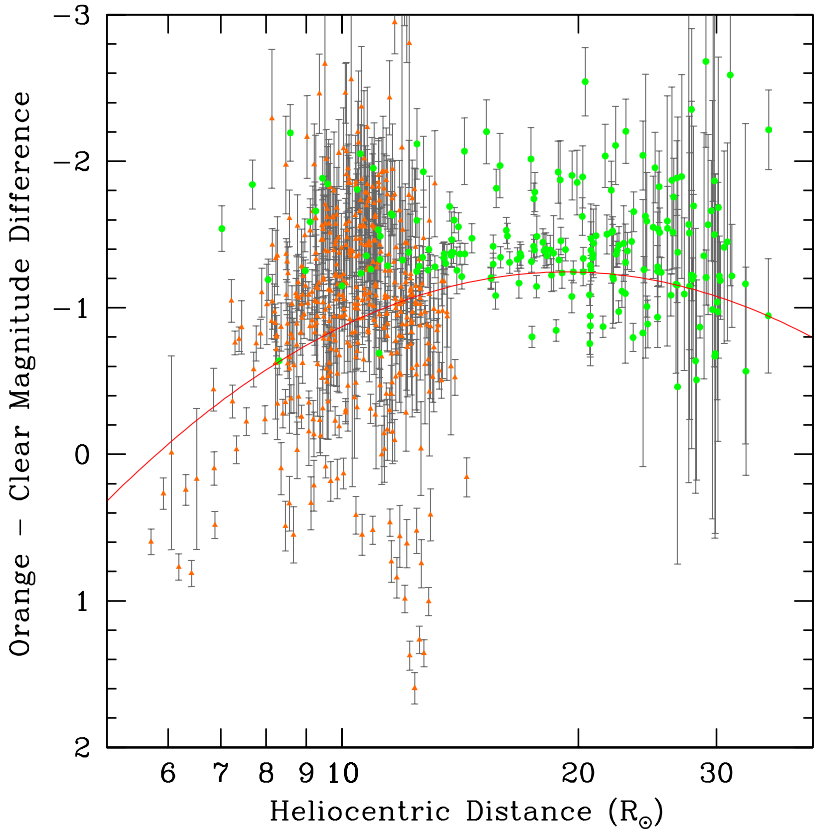

Fig. 8.— Orange – clear magnitude difference as a function of heliocentric distance. Negative values are brighter in the orange than the clear. The green circles are C3 orange – C3 clear magnitudes and the orange triangles are C2 orange – C3 clear magnitudes. The red line is the best fit quadratic to the data, which peaks at 18.6 $R_{\odot}$.

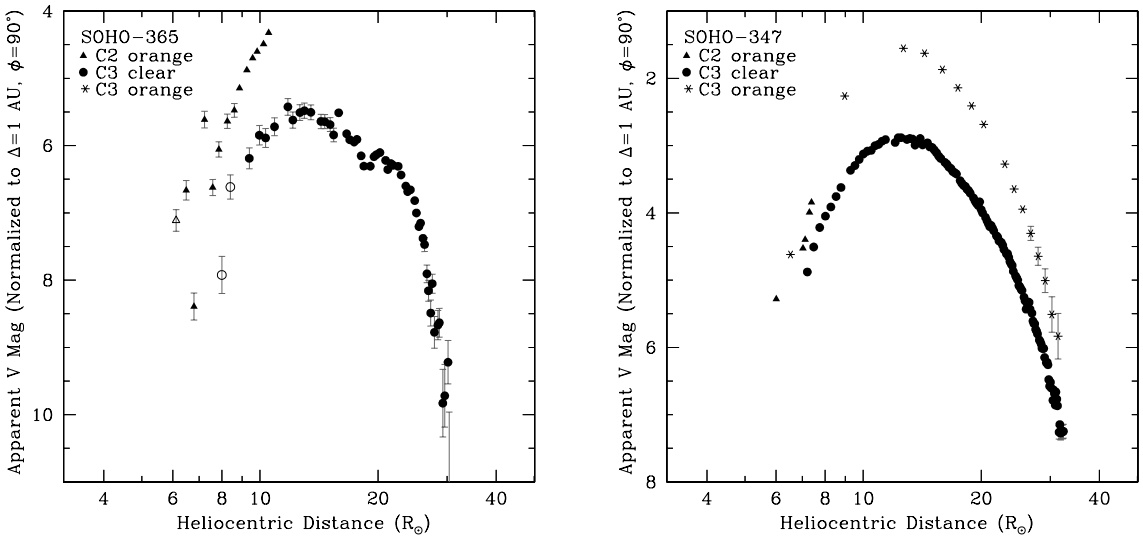

Fig. 9.— Lightcurves of Kreutz comets with overlapping orange and clear images. The left panel is C/2001 U7 (SOHO-365) and the right panel is C/2001 R2 (SOHO-347). The triangles are C2 orange images, the circles are C3 clear images, and the asterisks are C3 orange images. Open points signify images which have significant vignetting (greater than 4.0). Note that C/2001 R2 saturated the C3 detector at its peak, making the brightest points unreliable, and that the magnitude scales on the two panels are different. Error bars smaller than 0.1 magnitudes (for the upper error bar) have been suppressed.

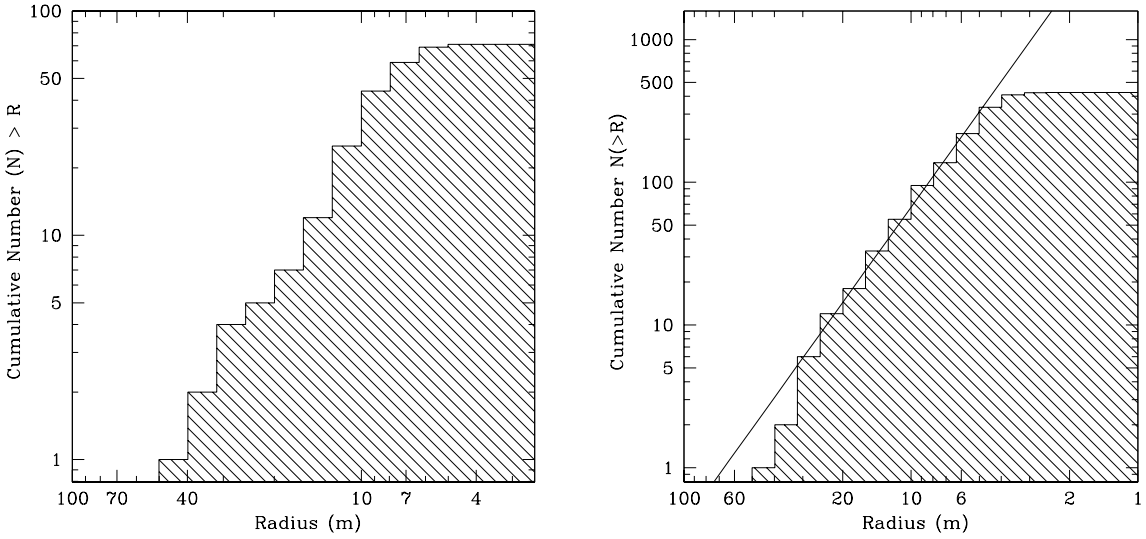

Fig. 10.— Cumulative size distribution of the comets with a discernible lightcurve peak in the C3 clear filter (left panel) and the cumulative size distribution based on the brightest point of all comets observed in the C3 clear filter between 10–15 $R_{\odot}$ (right panel). Both plots include the six comets which were omitted from the earlier discussion of peak distances because they saturated the detector (Section 5.1). These represent six of the seven points with sizes greater than 20 meters. The line in the right panel is a logarithmic fit from 5–35 meters in radius having a slope (log(number) vs. log(radius)) of −2.2.

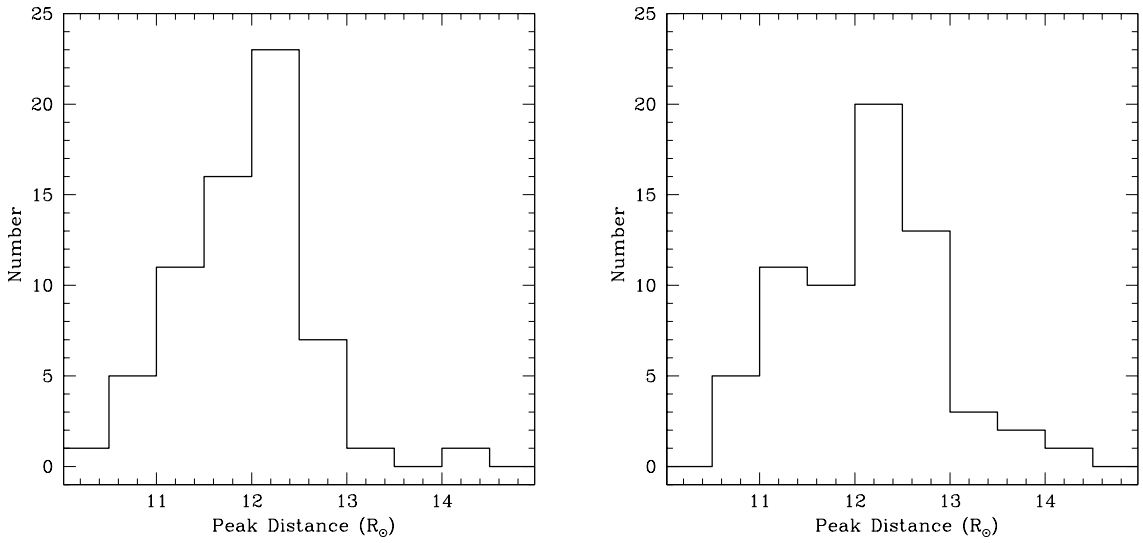

Fig. 11.— Histograms of the heliocentric distance of peak brightness for comets observed to peak in C3 for the uncorrected data (left panel) and the corrected data (right panel, which is identical to Figure 3).

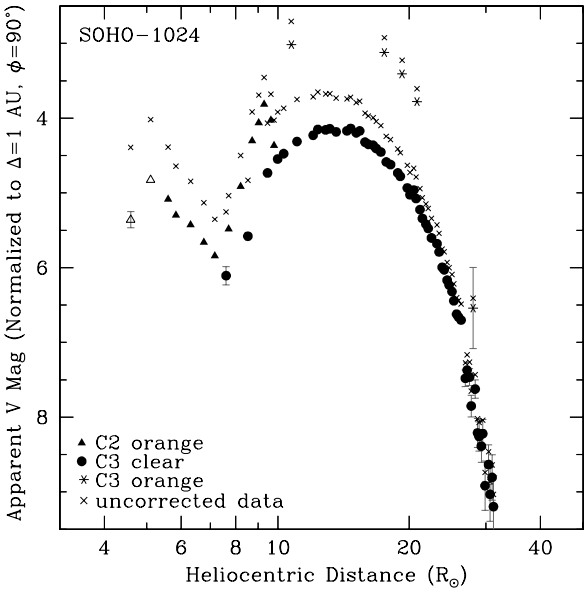

Fig. 12.— Lightcurve of C/2005 S1 (SOHO-1024) with and without photometric correction. The uncorrected data are plotted as crosses. The corrected data are plotted as triangles (C2 orange filter), circles (C3 clear filter), and asterisks (C3 orange filter). Open points are images with vignetting greater than 4.0. Error bars smaller than 0.1 magnitudes (for the upper error bar) have been suppressed.

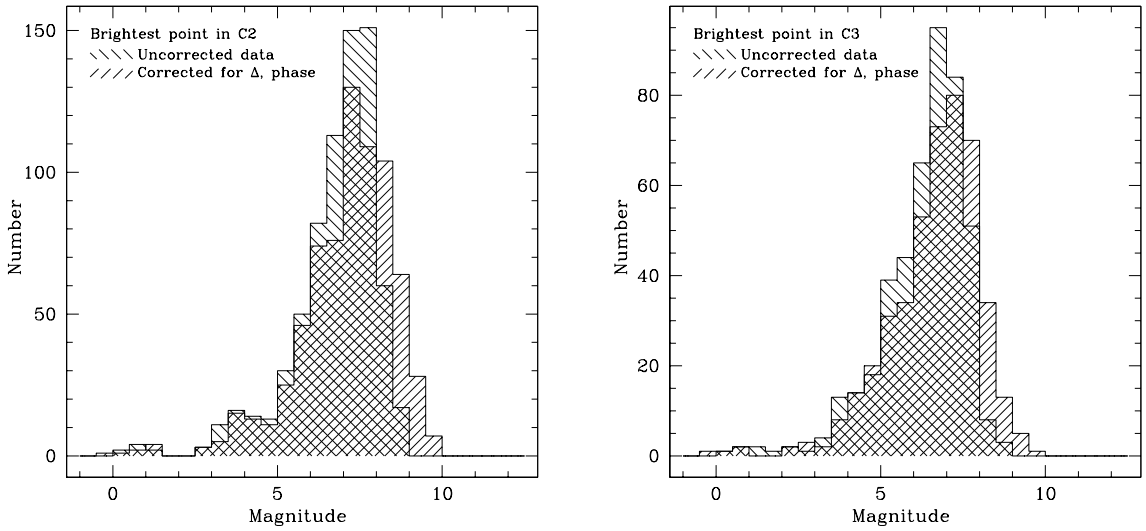

Fig. 13.— Histogram of brightest magnitude for comets observed in C2 (left panel) and C3 (right panel). The uncorrected size distribution has hatching going at $-45°$ and the data corrected for phase angle and SOHO-centric distance has hatching at $+45°$. Note that the scales are different because more comets are seen in C2 than in C3.

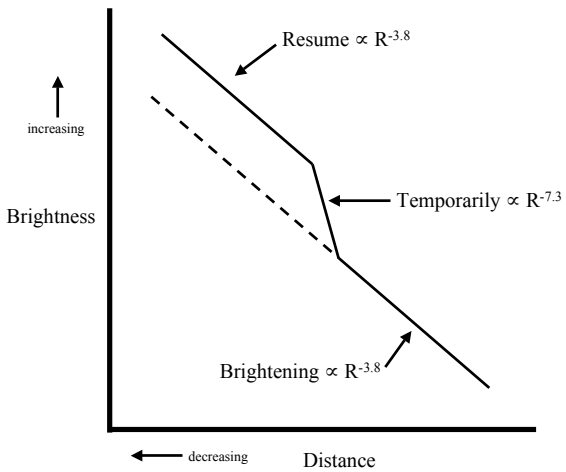

Fig. 14.— Illustration of the Kreutz brightening rate.

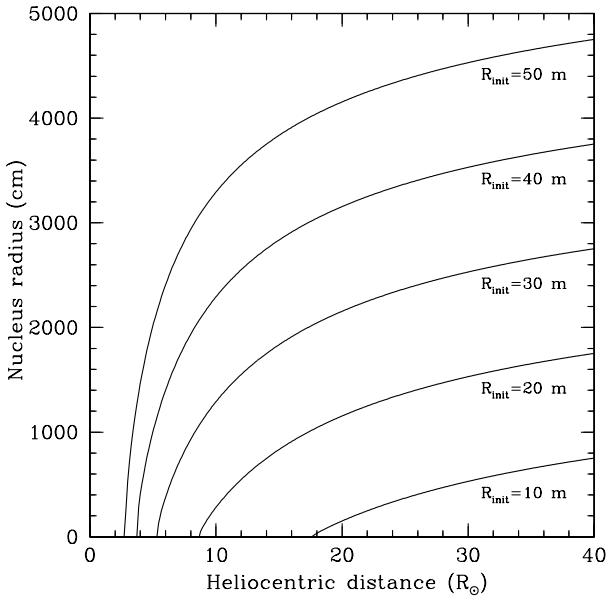

Fig. 15.— Decrease in size of a Kreutz nucleus due to water production. The initial sizes listed for each curve were the sizes 4 days prior to perihelion at a distance of $\sim$58 $R_\odot$. The comet follows the orbit of C/1963 R1 Pereyra which is very close to the "subgroup I" orbit (Marsden 1967) of most SOHO observed comets. The nucleus is assumed to be composed entirely of water, and the water production rate is scaled from 10^{18} molecules s^{-1} cm^{-2} at 1 AU by a factor r^{-2}.

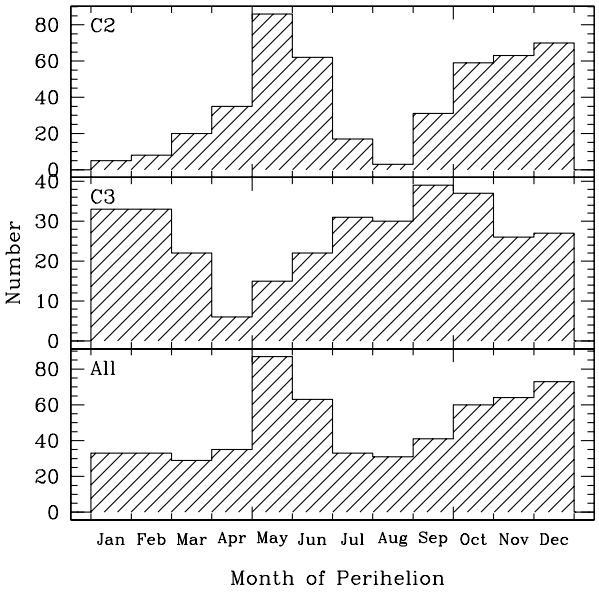

Fig. 16.— Histogram of the month of perihelion for Kreutz comets observed by SOHO from 2004–2007. The top panel shows comets observed in C2. The middle panel shows comets observed in C3. The bottom panel shows all comets observed, regardless of telescope. Note that the the total number of comets observed is less than the sum of the comets observed in C2 and C3 because many comets are seen in both telescopes. The period displayed (2004–2007) was chosen because it represents the most complete and uniform period of the dataset as discussed in Section 7.1.

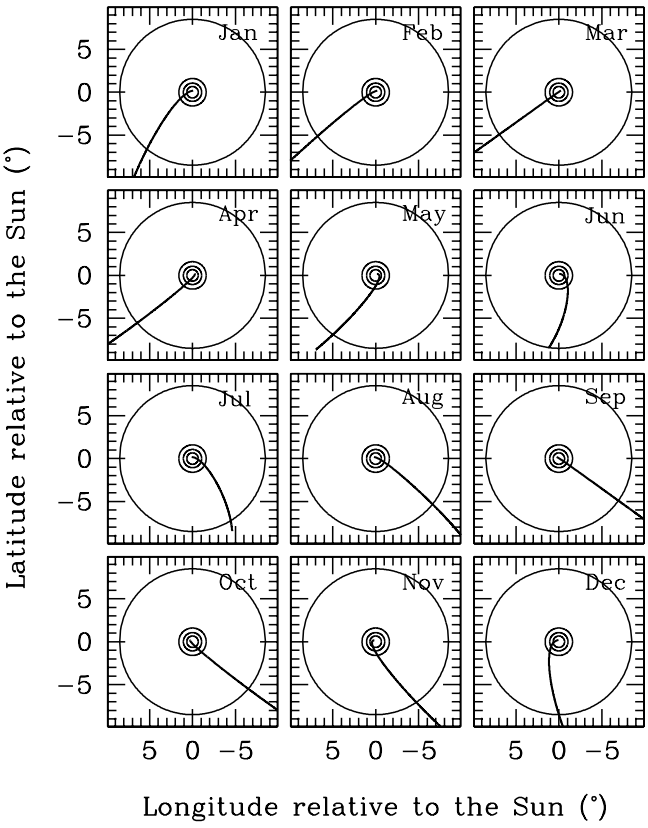

Fig. 17.— Monthly track across the SOHO coronagraphs for typical Kreutz comets. The track is for a comet which reaches perihelion on the 15^{th} day of the month specified in the upper right corner of each plot. The heavy line is the orbit prior to perihelion. The post-perihelion track is not plotted since no Kreutz comets have been seen by SOHO after perihelion. The circles represent the edges of the coronagraphs. Starting from the largest circle they are: C3 outer, C2 outer, C3 inner, C2 inner.

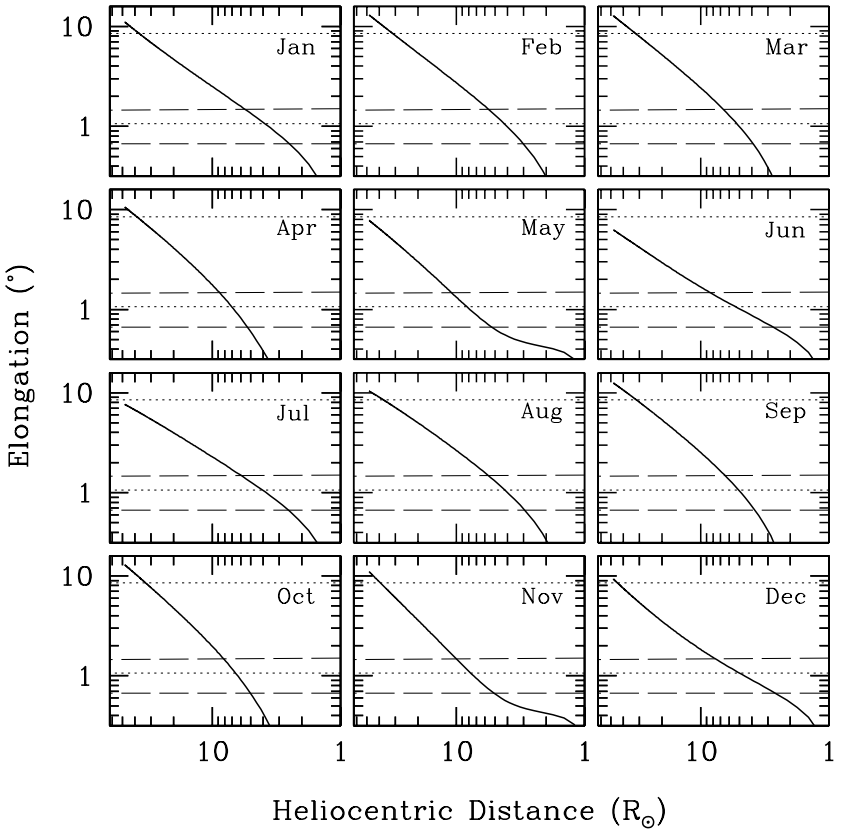

Fig. 18.— Solar elongation as a function of heliocentric distance for typical Kreutz comets. The orbit is for a comet which reaches perihelion on the 15^{th} day of the month specified in the upper right corner of each plot. The heavy line is the last 3 days of the orbit prior to perihelion. The post-perihelion track is not plotted since no Kreutz comets have been seen by SOHO after perihelion. The dotted and dashed horizontal lines denote the outer (upper) and inner (lower) radii of the C3 and C2 coronagraphs respectively.

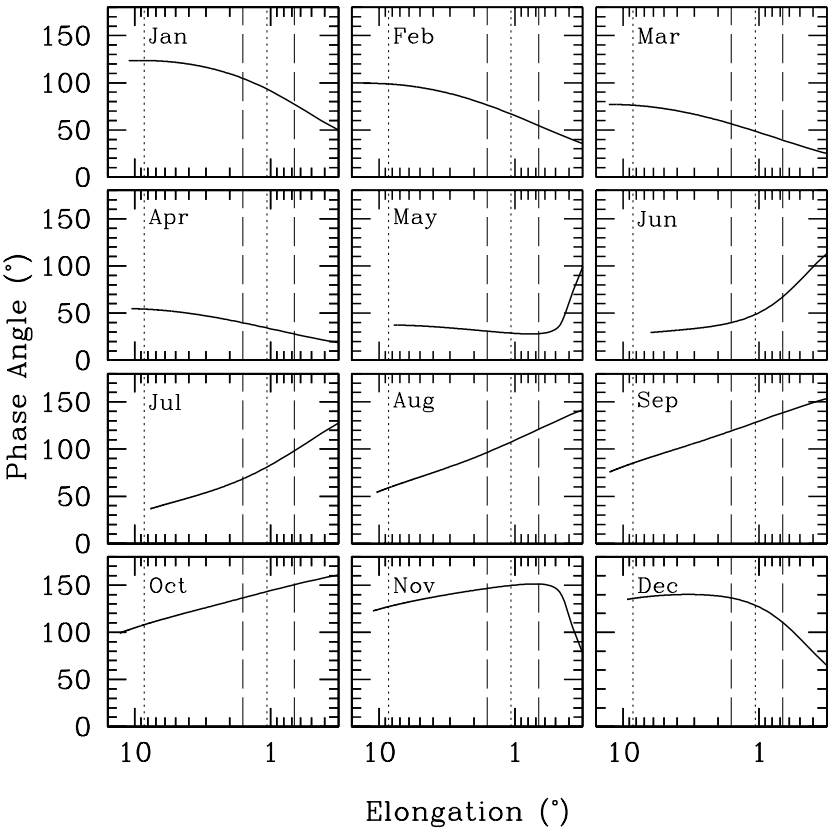

Fig. 19.— Monthly phase angle as a function of elongation for typical Kreutz comets. The phase angle is for a comet which reaches perihelion on the 15^{th} day of the month specified in the upper left corner of each plot. The heavy line is the phase angle prior to perihelion. The post-perihelion track is not plotted since no Kreutz comets have been seen by SOHO after perihelion. The dotted and dashed vertical lines denote the outer (left) and inner (right) radii of the C3 and C2 coronagraphs respectively.